Bias Evaluation and Reduction in 3D OP-OSEM Reconstruction in Dynamic Equilibrium PET Studies

Cláudia Régio Brambilla (c.regio-brambilla@fz-juelich.de)
Forschungszentrum Julich GmbH https://orcid.org/0000-0002-3735-8511

Jürgen Scheins
Forschungszentrum Julich GmbH

Ahlam Issa
Forschungszentrum Julich GmbH

Lutz Tellmann
Forschungszentrum Julich GmbH

Hans Herzog
Forschungszentrum Julich GmbH

Elena Rota Kops
Forschungszentrum Julich GmbH

N. Jon Shah
Forschungszentrum Julich GmbH

Irene Neuner
Forschungszentrum Julich GmbH

Christoph W. Lerche
Forschungszentrum Julich GmbH

Original research

Keywords: binding potential, dynamic PET, low statistics, neuroreceptor studies, quantitation bias

Posted Date: June 22nd, 2020

DOI: https://doi.org/10.21203/rs.3.rs-35926/v1

Bias Evaluation and Reduction in 3D OP-OSEM Reconstruction in Dynamic Equilibrium PET Studies

Cláudia Régio Brambilla[*1,2], Jürgen Scheins[1], Ahlam Issa[1], Lutz Tellmann[1], Hans Herzog[1], Elena Rota Kops[1], N. Jon Shah[1,3,4,5], Irene Neuner[1,2,4], Christoph W. Lerche[1]

[1]Institute of Neuroscience and Medicine, INM-4, Forschungszentrum Jülich GmbH, Wilhelm-Johnen-Straße, 52428 Jülich, Germany

[2]Department of Psychiatry, Psychotherapy and Psychosomatics, RWTH Aachen University, Pauwelsstraße 30, 52074 Aachen, Germany

[3]Institute of Neuroscience and Medicine, INM-11, Forschungszentrum Jülich GmbH, Wilhelm-Johnen-Straße, 52428 Jülich, Germany

[4]JARA – BRAIN – Translational Medicine, RWTH Aachen University, Pauwelsstraße 30, 52074 Aachen, Germany

[5]Department of Neurology, RWTH Aachen University, Pauwelsstraße 30, 52074 Aachen, Germany

*Corresponding author: Cláudia R. Brambilla – c.regio-brambilla@fz-juelich.de

Wilhelm-Johnen-Straße, 52428, INM-4 Forschungszentrum Jülich GmbH, Germany

Building: 15.16, Room: 1023 Tel.: +49 2461 61-96856 Fax: +49 2461-61-2089

j.scheins@fz-juelich.de

a.issa@fz-juelich.de

l.tellmann@fz-juelich.de

hans.r.herzog@gmx.de

e.rota.kops@fz-juelich.de

n.j.shah@fz-juelich.de

i.neuner@fz-juelich.de

c.lerche@fz-juelich.de

Abstract

Background: Iterative image reconstruction algorithms are widely used in positron emission tomography (PET). However, they are known to contribute to quantitation bias, which is particularly pronounced during dynamic PET studies such as neuroreceptor binding studies with ^{11}C-labelled radiotracers where count rates become low towards the end of the examination. This problem is relevant in case simultaneous PET/MR studies which apply a bolus-infusion protocol to allow the multimodal comparison between control or resting state and stimulation effects in a single session of e.g. 60 min, i.e. 3 half-lives of ^{11}C. A quantitation bias may interfere with stimulation related changes. In this study, we evaluated the impact of the 3D ordinary Poisson OSEM (3D OP-OSEM) on quantitation accuracy reconstructions and the subsequent propagation into binding potential values using a decay study of a ^{11}C filled phantom and a human brain data set. To evaluate the reconstruction bias, we tested different reconstruction framing schemes and propose a framing scheme that keeps the counts per time frame constant over the full acquisition time. We also compared the vendor's 3D OP-OSEM image reconstruction method to an *in-house* developed reconstruction (PRESTO toolkit).

Results: In general, a bias for low and high activity concentration regions was observed in the range of ± 3% and - 3% to 5%, respectively. Using the alternative proposed framing scheme, a lower bias was achieved for regions with low activity concentration using PRESTO, and a stabilization of the mean bias for the binding potential was achieved at around 5% with the vendor's reconstruction throughout the relevant activity curve time interval.

Conclusions: The bias in activity concentration propagated into the binding potential values leading to a mean bias of around 5%, thus allowing the detection of changes in binding values during equilibrium of $> 5\%$.

Keywords: binding potential, dynamic PET, low statistics, neuroreceptor studies, quantitation bias.

Background

Iterative image reconstruction algorithms based on the known maximum likelihood - expectation maximization (ML-EM) have been widely used in positron emission tomography (PET) for the past three decades, with the order-subset (OS) variants being particularly prevalent (1-4). However, these methods have been shown to cause bias for applications involving low count levels (5-9). This effect is often problematic in dynamic PET studies with ^{11}C-labelled radioligands and especially in the case of neuroreceptor binding studies that usually use reference regions, e.g. cerebellum or pons/brainstem, which frequently present low neuroreceptor concentrations levels and thus low counts of the radioligand per frame.

Other groups using ML-EM based reconstruction methods have reported different levels of bias (7) and overestimation, as well as underestimation in volumes of interest (VOIs) with either low or high activity concentrations (10). In the case of 3D OSEM based reconstruction algorithms, the source of the bias has been attributed to the introduction of a positive bias in the reconstructed images due to the non-negativity constraint in the data prior to correction (11). To avoid bias from the non-negativity constraint, 3D ordinary Poisson OSEM (OP-OSEM) can be used as an alternative iterative reconstruction method as it implements all required data corrections in a way that preserves non-negativity during the reconstruction (6, 12). However, 3D OP-OSEM uses observed random and scattered coincidence events without updating them for each iteration step during the image reconstruction (13). The accuracy of this method has been studied and a bias of 10% or more was reported (11) in regions of a homogeneous phantom. Byars and colleagues (14)

showed that the bias can be reduced when a variance reduction algorithm (VRR) is implemented to reduce the variance in estimated random counts. However, it is important to consider that other factors can also contribute to the bias in image reconstruction at low count rates, including scatter correction implementations (e.g. frame-based) or the framing scheme (10, 15, 16).

The aim of this study was to evaluate the impact of different framing schemes and reconstruction procedures on the quantitative accuracy of PET images using a ^{11}C filled phantom decay study and a bolus plus infusion (BI) human neuroreceptor study. Particular focus was given to the bias effects on the values of non-displaceable binding potential (BP_{ND}) at count rate situations normally found in dynamic [^{11}C]ABP688 (ABP) equilibrium PET studies. An alternative method for gathering the PET coincidences into a framing scheme is also proposed in which the counts per frame are kept at the same value for all reconstructed frames of the dynamic acquisition. As anticipated in (12, 16), the bias is dependent, in part, on the number of counts in the frame. This leads to the conclusion that the bias may be constant throughout the entire TAC when maintaining constant counts per frame over the entire time interval of the dynamic PET acquisition. Based on this premise, different framing schemes were also compared with respect to bias size and the limits of the bias range that a task must overcome in order to be effectively identified (how much change a task must induce to exceed the bias limits) were evaluated. Two spherical and one background VOIs from an adapted NEMA phantom were analyzed. The phantom had different dimensions, reflecting our BI protocol with ABP a glutamatergic receptor ligand with high and low neuroreceptor density regions to evaluate the limitations in binding quantification due to the bias. In addition, the bias obtained with the vendor's 3D OP-OSEM reconstruction was compared with the bias obtained with an *in-house* reconstruction (PRESTO (17)) both in the phantom study and with human data with ABP.

Methods

A. PET Acquisitions

All PET data (phantom and human brain studies) were acquired using a 3T hybrid MR-BrainPET insert system (SIEMENS, Erlangen, Germany) in list mode (18). The coincidences were corrected for random events using the delayed window technique with VRR, dead time, attenuation and scattered coincidences (single scatter simulation – SSS method), and physical decay. The image reconstruction was performed with the vendor-supplied 3D OP-OSEM (19) and *in-house* developed PRESTO implementations (2 subsets and 32 iterations, and 80 iterations respectively), with an isotropic voxel of 1.25 mm into a volume consisting of 153 transverse slices of 256 × 256 pixels. The vendor's reconstruction uses sinograms with span 9 axial data compression, whereas PRESTO is realized as a direct line of response (LOR) reconstruction without LOR data compression. Post-processing was performed with a 2.5 mm 3D Gaussian filter. Pmod software 3.9 was used to define the VOIs and to extract activity concentration (kBq/cm^3) for the analysis.

B. Phantom Study

An adapted NEMA phantom (20) with sphere inserts filled with ^{11}C was used and coincidence data were acquired during seven isotope half-lives, thus giving ~163 minutes total acquisition time for ^{11}C with its half-life $T_{1/2}$ = 20.38 minutes. An interval of $3T_{1/2}$, from 62 minutes to 122 minutes of the acquisition time was used for data analysis. This acquisition time interval was chosen according to the typical count rates measured in a human brain study with ABP alongside a BI protocol (see *Section C*) and a scan time of 65 minutes (~$3T_{1/2}$ of ^{11}C). The ratio of the activity concentration between the two spheres (Hot_1 with 28 mm of internal diameter and Hot_2 with 22 mm of internal diameter) and the background region (BG) was ~2:1. This value is frequently found for the ratio of activity concentrations in the grey matter cortex (GM) and cerebellar grey matter

(CER, reference region) during the steady-state condition in ABP studies. The activity concentrations for each time interval during the ^{11}C decay study with the phantom are given in Table 1.

TABLE 1
^{11}C DECAY EXPERIMENT WITH A PHANTOM (SELECTED TIME INTERVAL)

Time interval in multiples of $T_{1/2}$	**Phantom Regions (VOIs names)**	**^{11}C Activity Concentration (kBq/cm^3)**
T4	Hot1/Hot2	15.30
	BG	8.25
T5	Hot1/Hot2	7.65
	BG	4.13
T6	Hot1/Hot2	3.82
	BG	2.06

The half-life here is expressed as the number of elapsed ^{11}C half-lives during the decay experiment, where T4 is during the fourth $T_{1/2}$ (^{11}C) and so forth. The chosen T4, T5 and T6 were selected to represent typical activity concentration in human [^{11}C]ABP688 acquisitions.

A cold transmission scan of the adapted NEMA phantom using ^{68}Ge sources was acquired in a Siemens ECAT Exact HR+ PET scanner. This acquisition (2 bed positions with 20 minutes of transmission in a 256 × 256 matrix and reconstructed with OSEM 2D – 6 iterations and 16 subsets) was used to create the attenuation map for the phantom used in the ^{11}C decay study.

To obtain the ground truth data for the phantom study, the activity concentrations in the different phantom compartments were measured with a gamma counter (Wizard counter) repeating for 3 probes in a solution of 0.5 ml. Decay correction, counter calibration factor and volumes/weights of the probes were considered and standard corrections applied.

Figure 1 shows a PET image from ABP overlaid with an MR T1 image acquisition and a comparison to the image of an adapted NEMA phantom.

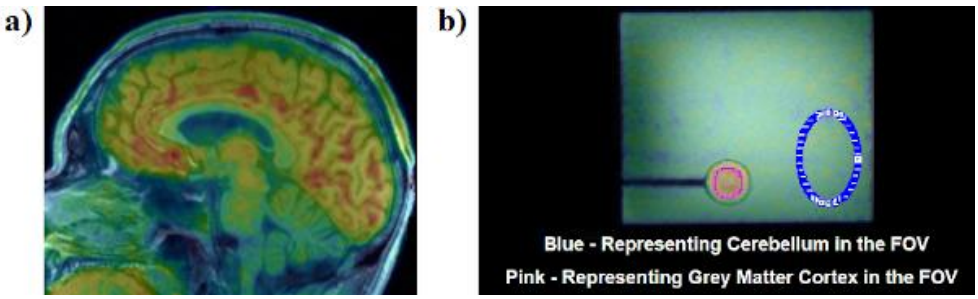

Fig. 1. a) Sagittal PET image from the ABP study overlaid with MR T1 image and **b)** Sagittal PET image of the NEMA phantom overlaid with an MR T1 image during the ^{11}C filled phantom decay study. The high activity concentration region (pink VOI) and low activity concentration region (blue VOI) is highlighted for bias analysis.

Based on the known neuroreceptor distribution of ABP, the background VOI (BG) was considered to be representative of CER as a reference region and the two hot sphere's VOIs (Hot_1 and Hot_2) were considered to be representative of the GM regions, i.e. parts of the cingulate cortex (neuroreceptor rich region in ABP, see *Section C*) and the nucleus accumbens. The latter is important for the analysis of psychiatric conditions, such as schizophrenia (21). The effective volumes of the three VOIs were: 112.86 ml (BG, 57782 voxels), 3.42 ml (Hot_1, 1751 voxels), and 1.13 ml (Hot_2, 578 voxels) respectively. To reduce partial volume effects in the analysis, the VOIs were drawn with a distance of 4 mm to the inner borders of the Hot_1 and Hot_2 spheres (effective internal diameters of 20 mm and 14 mm, respectively). Moreover, in the ^{11}C filled phantom decay study, following the application of all data corrections, a constant activity concentration was expected during the entire acquisition time (T1 to T7) in all phantom compartments since a BI study at equilibrium conditions aims to maintain constant activity concentrations in the brain compartments.

C. Human Study with [^{11}C]ABP688

PET Protocol with [^{11}C]ABP688: An analysis similar to that used in the phantom study was applied to already existing data from a dynamic PET acquisition on a subject with 437 MBq of totally administered activity of ABP. Details of this study can be found in (22). The radiosynthesis

of ABP was performed according to (23).

Applied BI protocol: The bolus injection had 50% of the total injected activity, followed by 65 minutes of infusion with 92 ml/h. The bolus injection was applied after positioning the subject in the scanner and began simultaneously with the start of PET data acquisition. A distribution equilibrium was observed at around 30 minutes after the bolus injection, and PET data acquisition stopped at 65 minutes with the end of the infusion. The emission data were corrected for attenuation using template-based methods (24). Head motion was corrected with a frame-by-frame realignment to a reference image (frame length 5 minutes post-injection) and was performed with Pmod 3.9. Head motion was lower than 1 mm, which is less than the PET spatial resolution of 3 mm at the center of the FOV. VOIs were selected in CER, anterior cingulate cortex (ACC) and posterior temporal cortex (Post-Tl), as the last two regions have a high density of metabotropic glutamatergic receptors type 5 (mGluR5) (25).

D. Reconstruction – Frame Schemes

The different framing schemes used to test bias in the time activity curves (TACs) and binding potential values were defined by either constant or increasing frame lengths, as well as an alternative framing scheme with variable frame lengths that takes the decreasing count rate during the dynamic PET into account. The framing schemes for the phantom study and the human brain study were defined as follows:

Constant Frame Length Schemes (Const): PET list-mode data of the entire acquisition was sorted into time frames with constant frame lengths of 2, 3 or 5 minutes respectively (Const 2 min, Const 3 min and Const 5 min).

Increasing Frame Length Scheme (Incr): PET list-mode data was sorted into time frames with increasing frame length, i.e. during T4 the frame length was set to 2 minutes and during T5 and

T6 the frame length was set to 3 minutes and 5 minutes (Incr 2-3-5 min), respectively. In this way, the lower counts for later frames caused by the radioactive decay of ^{11}C was compensated to some extent.

Increasing Frame Length Scheme with Constant True Counts (Const Trues): True events versus time curves were extracted from the acquisition and the frame lengths were adjusted to values which yielded the same total counts per frame for all frames of the dynamic PET data. The number of counts in the final frame of the acquisition was taken as a reference for counts per frame. Earlier frames were accordingly shorter. A duration of 5 minutes was chosen for the final frame since this is a typical setting for applications with cognitive tasks in simultaneous PET/MR applications and our BI protocol. The three framing schemes were evaluated with both reconstructions.

We would like to emphasize here that the advantage of the BI protocol in our case is the simplicity over the dual-bolus injection approach, because it allows us to measure the baseline and challenge effects in BP_{ND} in a single acquisition session. Another important point is the simultaneous use of other imaging or monitoring modalities, such as magnetic resonance (MR) or electroencephalography (EEG) at the same brain state condition. Our presented approach can also be applied to pure bolus or pure infusion protocols since the bias in estimated binding values, is not caused by the activity application protocol, but the image reconstruction itself. However, the bias reduction for parameters estimated with kinetic modeling still needs to be evaluated in an follow up study.

E. Bias Analysis

Bias and variability were analyzed as follows:

Activity Concentration Accuracy: The bias of the measured activity concentration ($A_{measured}$) was computed by (1):

$$\text{Bias } [\%] = \left[\frac{(A_{measured} - A_{true})}{A_{true}}\right] \times 100 \quad (1)$$

where A_{true} is the true activity concentration from the probes measured in the gamma counter (ground-truth value) and $A_{measured}$ is the mean activity concentration in the VOIs representing the cerebellum (blue VOI in Figure1(b)) or hot spheres (pink Hot_1VOI as an example in Figure1(b)) in each frame. PRESTO was cross-calibrated to the vendor's 3D OP-OSEM reconstruction with respect to the activity concentration accuracy. Box plots were used to represent the bias variability of the measurements for each VOI, for the different acquisition intervals T4, T5, T6, and for the different framing schemes.

Binding Potential Accuracy: The procedure described above in (1) was also used to estimate the bias and variability of the binding potential values (BP), by considering BP instead of the activity concentration A. The BP_{true} (for Hot_1 and Hot_2) values were estimated as presented in (2). Equation 3 was used to calculate $BP_{measured}$.

$$BP_{True} = \left[\frac{A_{TrueHot}}{A_{TrueBG}}\right] - 1 \quad (2)$$

$$BP_{Measured} = \left[\frac{A_{VOI1}}{A_{VOI2}}\right] - 1 \quad (3)$$

where A_{VOI1} is the mean activity concentration in the VOI_1 (high activity concentration region – Hot_1 or Hot_2 for the phantom and ACC or Post_Tl for human data) and A_{VOI2} is the mean activity concentration in the VOI_2 (low activity concentration region – representing BG for the phantom or CER for human data). Again, box plots were used to represent the variability of the BP values

for the different framing schemes, time intervals and regions. BP was used for the phantom study and BP_{ND} was used for the human study (binding potential values).

Linear Fit and Slope: TACs recorded in the phantom and human brain studies were also analyzed by evaluating the slope of a straight line fitted to the data. The percentage change per hour [%/h] of the TACs were evaluated for the equilibrium interval (human study) or the time intervals T4, T5 and T6 (phantom study) and compared. By choosing the Const Trues framing scheme, we hypothesized that the same bias would always be obtained throughout the TACs. Thus, the bias should not change the slope of the TACs. However, bias from framing schemes that do not consider constant true counts per frame, such as Const or Incr schemes, may show different slope values between the time intervals and higher slope values in the human data study.

Standard error (SE): Statistical SE was computed according to (4) and Gaussian error propagation was used to estimate the SE for the BP values.

$$\mathrm{SE}[\%] = \left[\frac{\sigma}{\sqrt{n}}\right] \times 100 \tag{4}$$

where σ is the standard deviation in the VOI regions and n is the number of pixels from the VOI. This analysis was performed for both reconstructions.

Results

A. *Phantom Study*

Activity Concentration Accuracy: Figure 2 shows the relative bias for the three regions in the phantom, for the intervals T4, T5 and T6, and for the three different Const framing schemes explained in *Section D.*

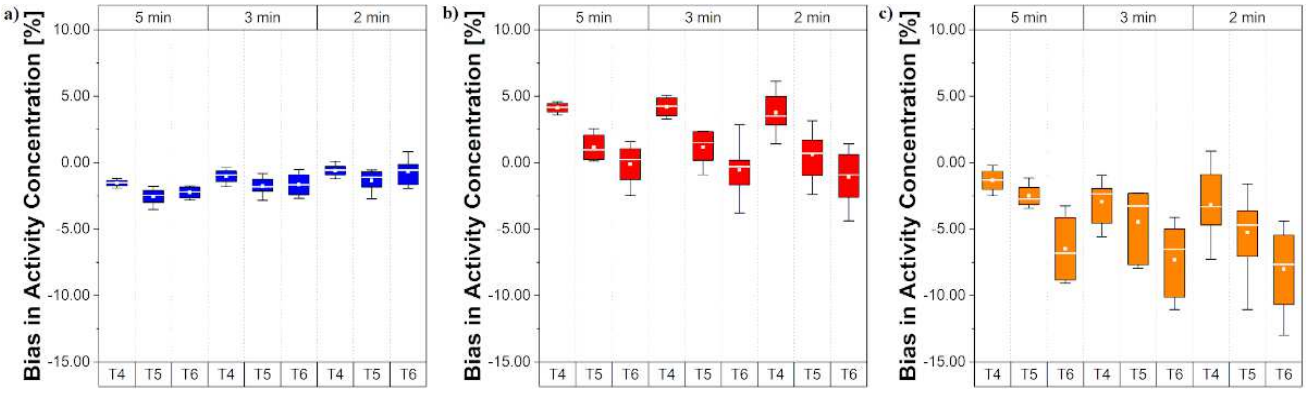

Fig. 2. Bias and variability in activity concentration for **a)** BG region (low activity concentration), **b)** Hot_1 region (high activity concentration) and **c)** Hot_2 region (high activity concentration); all with vendor's reconstruction.

In Figure 2 a) it is possible to notice a slightly increased bias in the BG region with decreasing frame length (lower count statistics per frame). In contranst, an opposite behaviour is shown in hot regions in b) and c) where the bias becomes negative with decreasing frame length. Figure 3 compares the relative errors for the three phantom regions, for the three intervals T4, T5 and T6, and for the Const 5 min framing scheme, the Incr and Const Trues schemes (described in S*ection D*).

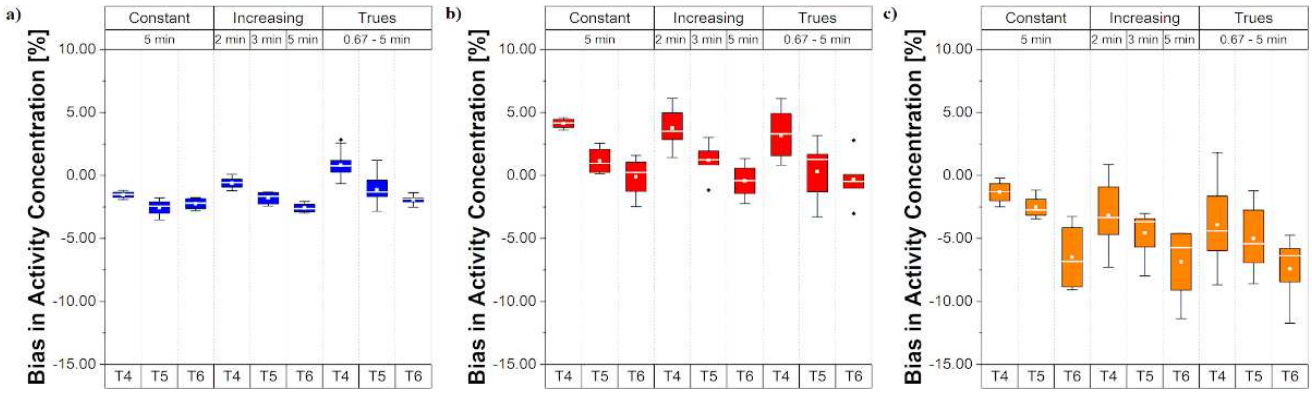

Fig. 3. Bias and variability in activity concentration for different framing schemes **a)** BG region (low activity concentration), **b)** Hot_1 region (high activity concentration) and **c)** Hot_2 region (high activity concentration); all with vendor's 3D OP-OSEM reconstruction.

A similar trend for the BG region can be noticed in terms of increased bias with decreasing frame length, but this time with reduced bias in T6 and the opposite behavior for Incr and Const Trues schemes is seen. In the hot regions, the negative bias is maintained, but again there is a reduced bias in the T6 time interval for Incr and Const Trues schemes compared to Const schemes, especially with the Const Trues scheme.

Binding Potential Accuracy:

Figure 4 presents the relative errors of BP values in the two hot phantom VOIs for different framing schemes and time intervals.

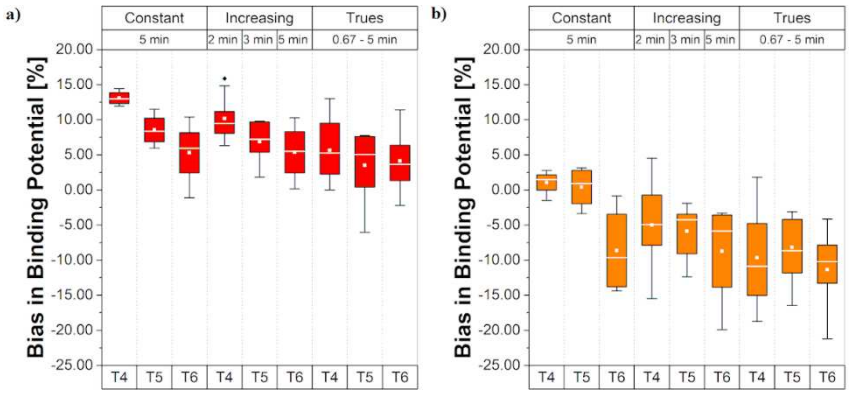

Fig. 4. Bias and variability of BP values for **a)** Hot_1 region, and **b)** Hot_2 region; all with vendor's 3D OP-OSEM reconstruction.

Note that, for the scheme with Const 5 min framing, the bias became variable within the time interval (from 12% to 5% for Hot_1 and from 1% to -10% for Hot_2), suggesting a different bias range according to the time intervals during the acquisition. This trend is minimized when Incr 2-3-5 min and Const Trues framing schemes were used and the bias range remained even closer in the all-time interval with the Const Trues scheme (Figure 4 a) bias around 5% in all-time interval and b) bias around -10% in all-time interval). However, in the Hot_2 region, the bias became higher negative and with higher variability, especially in the T6 interval for all schemes tested (up to - 10%) even with the proposed framing Const Trues. It is important to bear in mind that these data were not corrected for partial volume effects (PVE). However, the maximum estimated effect is around 15%-17% and the estimated correction factor is around 0.84 for the reported activity concentration values (hot regions are 4 cm far away from the FOV center). The PVE can be expected to be the same size for all framing schemes and time intervals. PVE was estimated with a geometric transfer matrix (GTM) using Pmod.

Time Activity Curves and Fit Analysis:

As shown in Figure 5 for four different framing schemes, the TACs of VOIs (BG and Hot_1) were approximated separately by individual linear fits for the intervals T4, T5 and T6. Hot_2 will no longer be shown since a larger bias and variability for quantification was noticed in this region. The BP values became particularly unreliable and we do not intend to analyze such small region in our BI protocol in the future due to the complexity of task effects analysis. A similar trend found in Figure 5. can be seen in the box plots (Figure 2 and Figure 3), which show a negative slope for the BG region in T4 and T5 and positive slopes in T6 (more pronounced in Const schemes). Note the negative slopes in the Hot_1 region for different framing scheme methods. Slope values ± SE for the decay corrected TACs are outlined in Table 2.

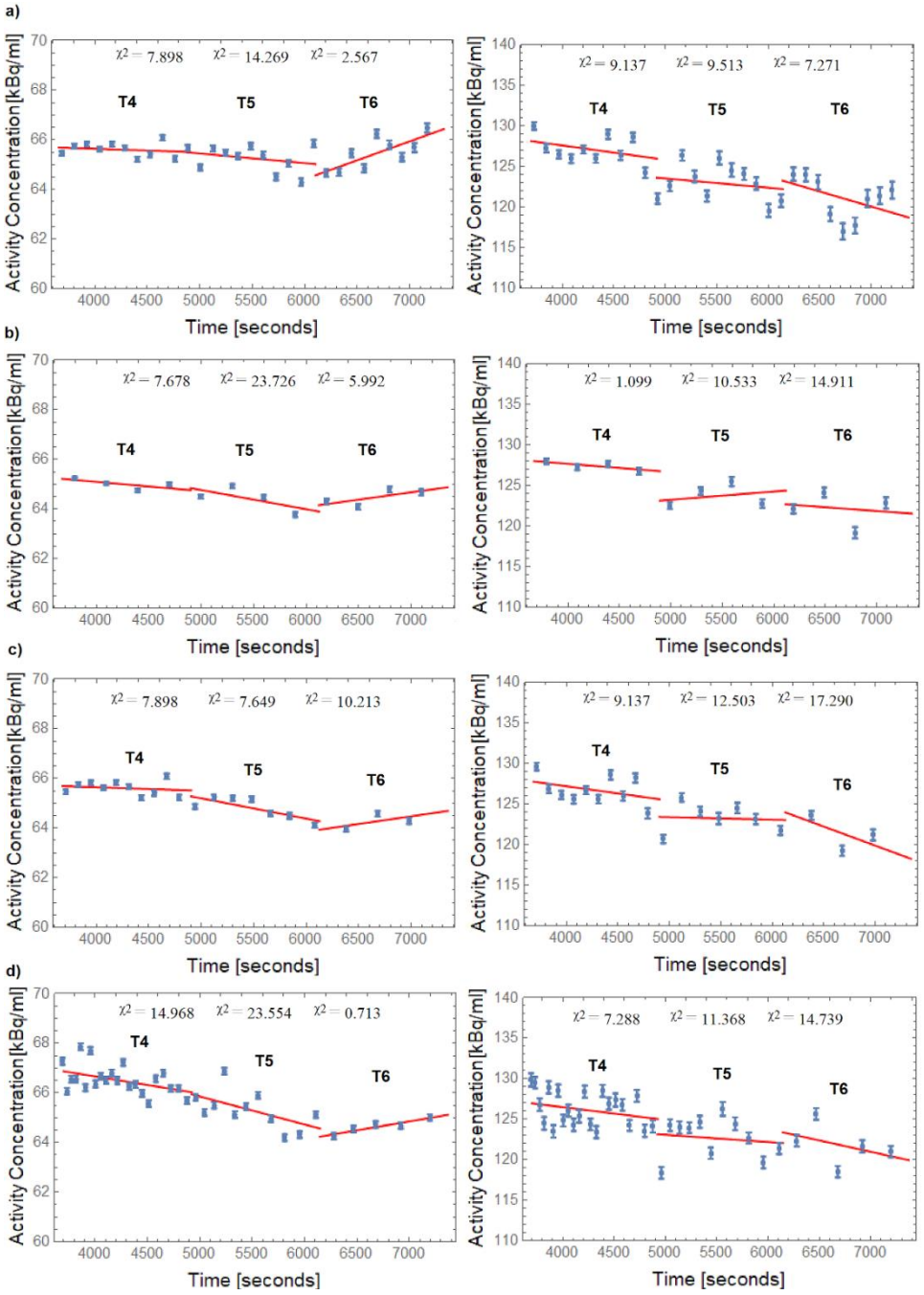

Fig. 5. TACs and linear fits for BG (left side) and Hot_1 (right side) regions for **a)** Const 2min, **b)** Const 5min, **c)** Incr 2-3-5 min and **d)** Const Trues; all with vendor's 3D OP-OSEM reconstruction. χ^2: goodness of linear fit.

TABLE 2
TIME ACTIVITY CURVES – SLOPE* RESULTS – PHANTOM DATA

Frame Scheme	Half-Life ($T_{1/2}$)	Slope ± SE (%/h) BG	Slope ± SE (%/h) Hot1
Const 2 min	T4	-0.8 ± 1.4	-5.0 ± 4.3
	T5	-2.1 ± 2.2	-3.4 ± 5.2
	T6	8.4 ± 2.7	-11.1 ± 8.1
Const 5 min	T4	-2.1 ± 1.5	-2.9 ± 1.7
	T5	-4.3 ± 3.5	2.9 ± 6.7
	T6	3.3 ± 2.3	-2.8 ± 10.7
Incr 2-3-5 min	T4	-0.8 ± 1.4	-5.0 ± 4.3
	T5	-4.5 ± 1.6	-0.9 ± 5.7
	T6	3.5 ± 4.8	-13.9 ± 17.3
Const Trues	T4	-3.7 ± 1.8	-4.5 ± 3.6
	T5	-6.2 ± 2.9	-2.6 ± 5.9
	T6	4.0 ± 0.8	-8.3 ± 11.1

*Slope – Linear fits from graphs presented in Figure 5, and SE – Standard Error.

B. Application to a Human Brain Study Data

For human brain studies, the true activity concentrations in brain regions and the binding potential values are not known. Therefore, here, the TACs during the equilibrium phase of the acquisition were directly analyzed using linear fits (Figure 6) to compare the reconstruction bias of the different framing schemes. Table 3 shows the corresponding slope results (%/h ± SE).

TACs Analysis for [^{11}C]ABP688:

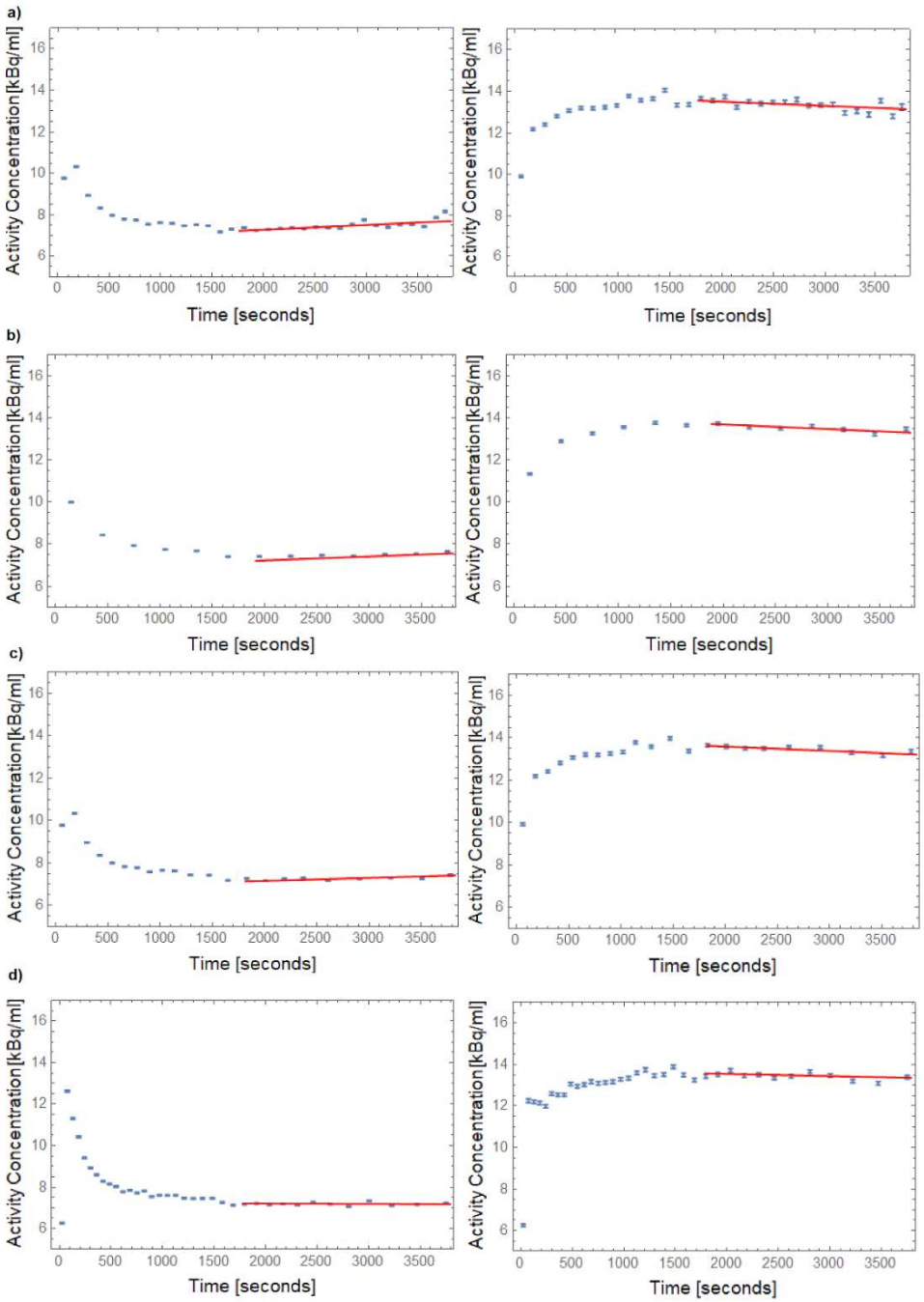

Fig. 6. TACs and linear fits during equilibrium in CER (left side) and ACC (right side) regions from a human brain study for **a)** Const 2 min, **b)** Const 5 min, **c)** Incr 2-3-5 min and **d)** Const Trues; all with vendor's 3D OP-OSEM reconstruction.

TABLE 3

TIME ACTIVITY CURVES - SLOPE* RESULTS – HUMAN DATA

Frame Scheme	Slope ± SE (%/h) CER	Slope ± SE (%/h) ACC
Const 2 min	12.3 ± 2.8	-7.7 ± 2.0
Const 5 min	5.3 ± 1.0	-4.7 ± 1.7
Incr 2-3-5 min	3.4 ± 1.6	-5.1 ± 1.1
Const Trues	0.6 ± 1.9	-4.9 ± 1.9

*Slope – Linear fits from graphs presented in Figure 6, and SE – Standard Error.

Using the human brain data, it is again possible to confirm the bias behavior for low activity concentration regions as CER and high activity concentration regions as ACC (see Figure 6 and Table 3). Please note the higher slope values in CER when using Const framing methods and its reduction when applying the proposed Const Trues framing scheme method (results using vendor's reconstruction).

BP values with [^{11}C]ABP688:

The effects of the different framing schemes on BP_{ND} values are shown in Figure 7. Here the effects of bias propagation into BP_{ND} values is clearly noticeable, especially after 3000 seconds for the Cont 2 min framing schemes. Note the reduction in the bias when Incr 2-3-5 min and Const Trues time length schemes were used.

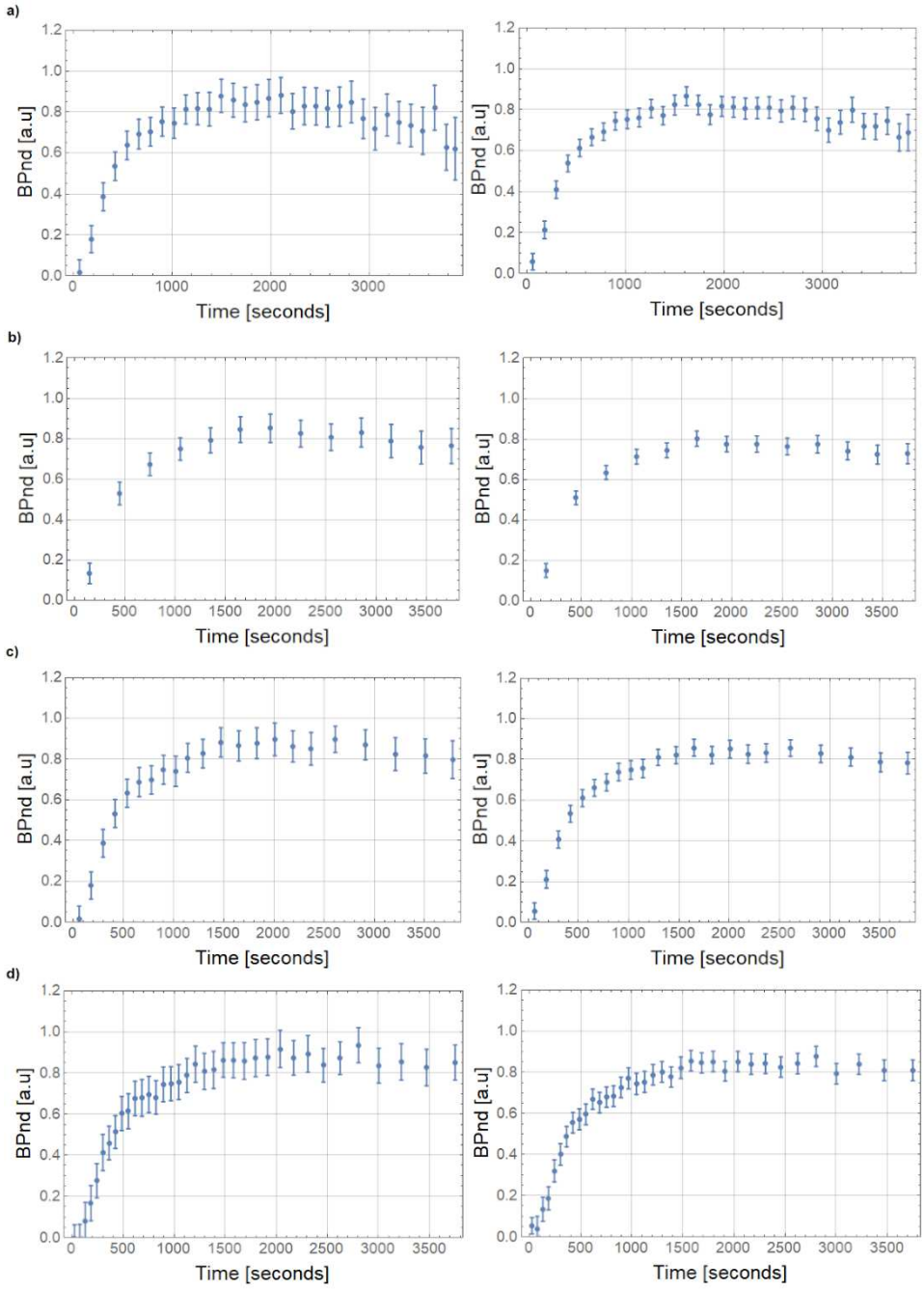

Fig. 7. Values of BP_{ND} ± SE for ACC (left side) and Post-Tl (right side) in a human brain study for **a)** Const 2 min, **b)** Const 5 min, **c)** Incr 2-3- 5 min and **d)** Const Trues; all with vendor´s 3D OP-OSEM reconstruction.

C. PRESTO Comparison

Phantom Study:

Activity Concentration and Binding Potential Accuracy:

For simplicity, the different framing schemes for each reconstruction procedure are shown for comparison in Figure 8.

In the comparison between both reconstruction procedures, PRESTO shows no significant rising behavior in the T6 time interval for BG in the Const 5 min framing scheme (see Figure 8.a)). For the Hot_1 region (Figure 8.b)), the bias is higher, but it is possible to notice that the mean biases are closer to each other for T5 and T6 time intervals, and the spread of the mean bias values from the vendor's reconstruction is slightly higher in the same time interval. Similar behavior is also shown in the BP bias values, but this time when the Const Trues framing scheme is applied, the vendor's reconstruction shows lower mean bias values (around 5%) during the entire time interval (T4, T5, and T6) against 10% from PRESTO.

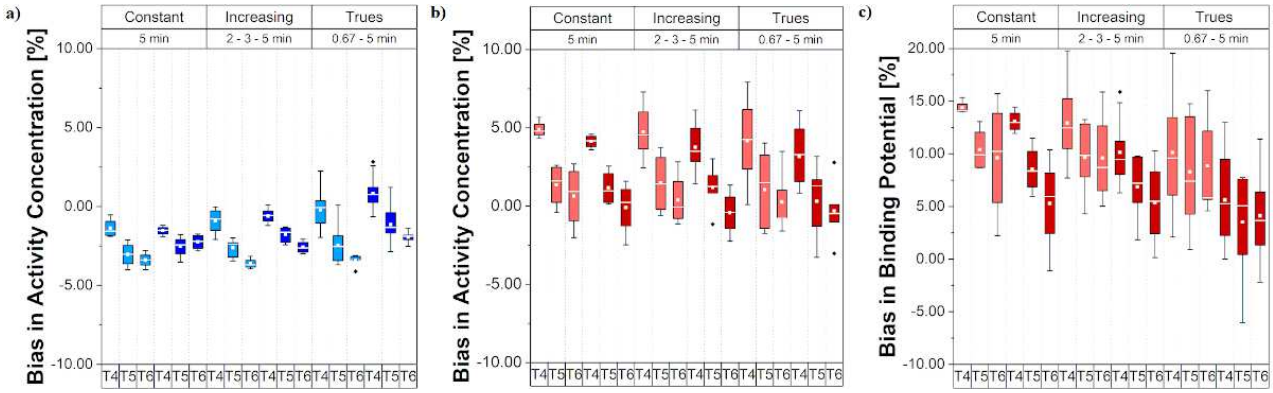

Fig. 8. Bias in activity concentrations and BP values for different framing schemes comparing PRESTO (light blue, light red) and vendor's 3D OP-OSEM (dark blue, dark red) in **a)** BG, **b)** Hot_1 and **c)** Hot_1 BP.

Time Activity Curves and Fit Analysis:

Slope values for the different framing schemes with PRESTO reconstruction are presented in Table 4, per half-life and phantom regions as shown in Figure 6 and Table 2 for comparison with

vendor's 3D OP-OSEM reconstruction. TACs can be seen in the supplementary file[1].

TABLE 4
TIME ACTIVITY CURVES - SLOPE* RESULTS – PHANTOM DATA - PRESTO

Frame Scheme	Half-Life ($T_{1/2}$)	Slope ± SE (%/h) BG	Slope ± SE (%/h) Hot_1
Const 2 min	T4	-5.0 ± 1.6	-5.8 ± 5.5
	T5	-4.2 ± 2.2	-8.4 ± 5.8
	T6	4.7 ± 2.7	-12.7 ± 9.4
Const 5 min	T4	-5.5 ± 1.8	-4.8 ± 1.4
	T5	-5.2 ± 3.6	-3.7 ± 8.3
	T6	1.7 ± 3.2	-0.12 ± 13.3
Incr 2-3-5 min	T4	-5.0 ± 1.6	-5.7 ± 5.5
	T5	-5.5 ± 1.1	-5.7 ± 6.3
	T6	2.2 ± 4.6	-17.0 ± 17.8
Const Trues	T4	-6.0 ± 1.8	-7.6 ± 4.7
	T5	-5.8 ± 3.0	-10.5 ± 6.0
	T6	3.5 ± 1.4	-12.2 ± 9.2

*Slope – Linear fits from PRESTO reconstructed data, and SE – Standard Error.

Human Study:

TACs Fit Analysis with [^{11}C]ABP688:

The evaluation explained in *Section D* was repeated for the PRESTO reconstruction and the results are given in Figure 9 and Table 5.

[1] PRESTO TACs and linear fits for BG, Hot_1 regions and x^2 goodness of linear fit are available in supplement.

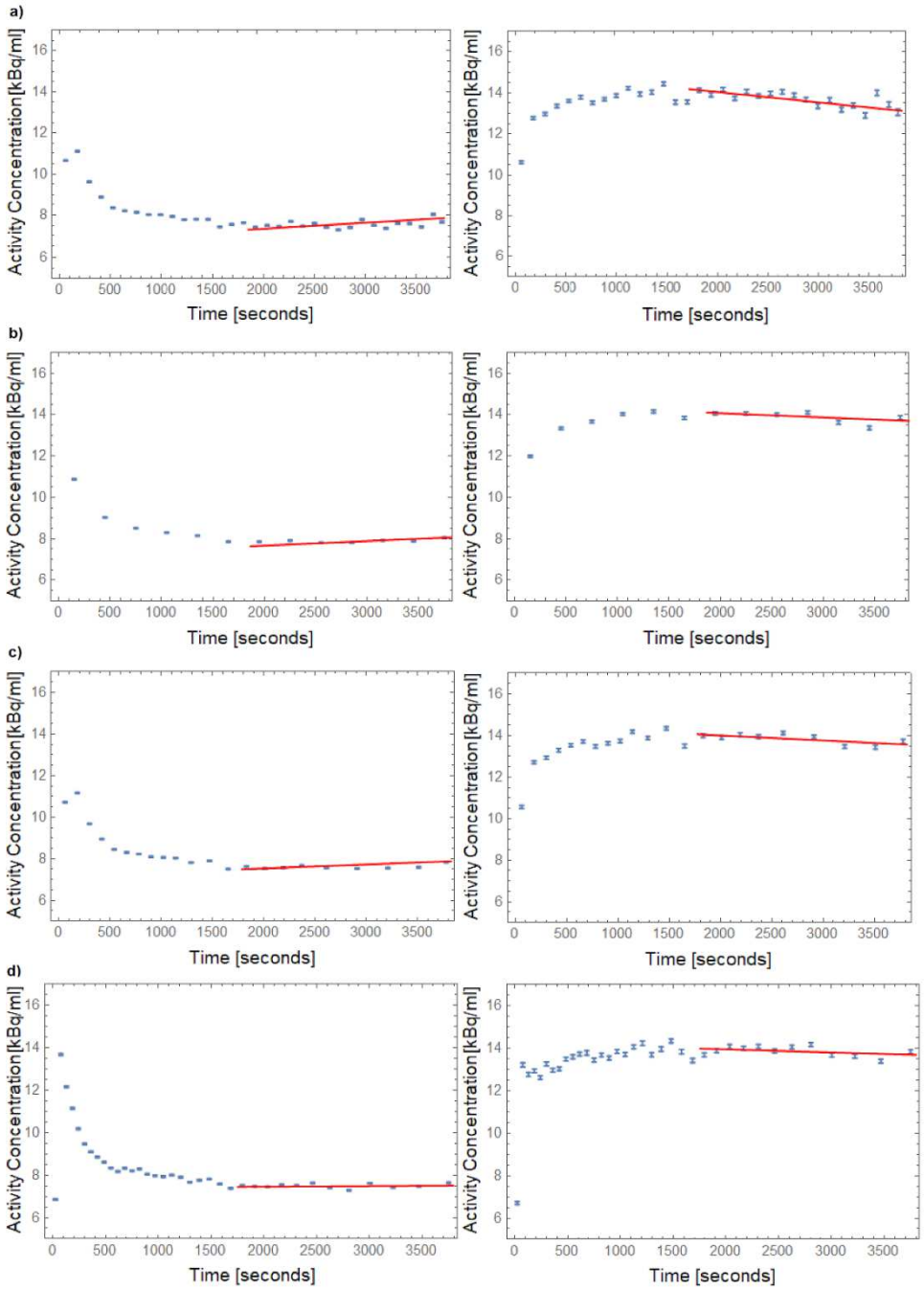

Fig. 9. TACs and linear fits during equilibrium in CER (left side) and ACC (right side) regions from a human brain study for **a)** Const 2 min, **b)** Const 5 min, **c)** Incr 2-3-5 min and **d)** Const Trues; all with PRESTO reconstruction.

TABLE 5
TIME ACTIVITY CURVES - SLOPE* RESULTS – HUMAN DATA - PRESTO

Frame Scheme	Slope ± SE (%/h) CER	Slope ± SE (%/h) ACC
Const 2 min	4.0 ± 3.0	-11.6 ± 2.6
Const 5 min	3.4 ± 1.8	-7.4 ± 3.2
Incr 2-3-5 min	2.9 ± 2.1	-6.7 ± 2.2
Const Trues	1.5 ± 2.5	-6.2 ± 2.4

*Slope – Linear fits from graphs presented in Figure 9, and SE – Standard Error.

Comparisons between the vendor's 3D OP-OSEM reconstruction (see Figure 6 and Table 3) and PRESTO are possible by looking at the slope values in BG and CER low activity concentration regions. As already shown in the box plots (Figure 8 a)), it is possible to achieve lower slope values in these regions using PRESTO reconstruction. However, higher bias in Hot_1 and ACC regions was also shown for PRESTO.

BP_{ND} values with [^{11}C]ABP688:

Figure 10 presents BP_{ND} values using PRESTO reconstruction and Table 6 shows the slope from the BP_{ND} curves for the different framing schemes and for both reconstruction procedures during the equilibrium phase (from 1800 seconds to the acquisition end).

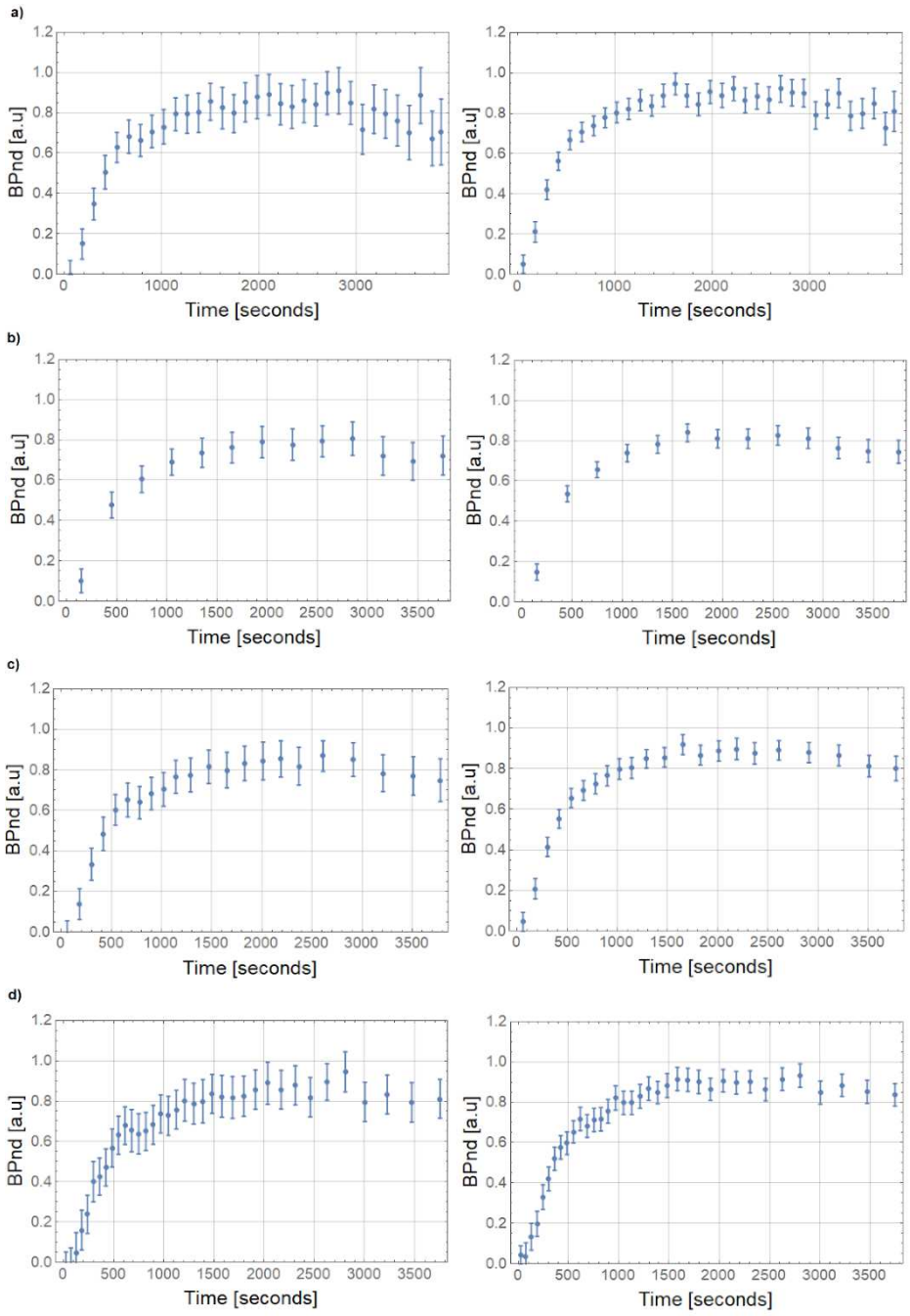

Fig. 10. Values of BP_{ND} ± SE values for ACC (left side) and Post-Tl (right side) regions from a human brain study for **a)** Const 2 min, **b)** Const 5 min, **c)** Incr 2-3-5 min and **d)** Const Trues; all with PRESTO reconstruction.

TABLE 6

BP_{ND} CURVES SLOPES* RESULTS – HUMAN DATA - VENDOR'S 3D OP-OSEM

Frame Scheme	Slope ± SE (%/h) ACC	Slope ± SE (%/h) Post-Tl
Const 2 min	-39.3 ± 6.4	-29.8 ± 4.3
Const 5 min	-20.10 ± 3.1	-16.5 ± 2.2
Incr 2-3-5 min	-15.20 ± 3.9	-12.8 ± 3.0
Const Trues	-7.7 ± 5.0	-6.1 ± 3.9

BP_{ND} CURVES SLOPES* RESULTS – HUMAN DATA - PRESTO

Frame Scheme	Slope ± SE (%/h) ACC	Slope ± SE (%/h) Post-Tl
Const 2 min	-24.2 ± 8.2	-22.6 ± 5.4
Const 5 min	-17.2 ± 7.2	-20.1 ± 3.6
Incr 2-3-5 min	-14.7 ± 6.1	-17.5 ± 3.6
Const Trues	-7.3 ± 7.7	-10.2 ± 4.3

*Slope – Linear fits from graphs presented in Figure 7 and Figure 10, SE – Standard Error.

Discussion

In this study, the quantification bias given by different framing schemes was investigated. In addition, an alternative framing scheme (Const Trues) that kept constant true counts per frame in all of the PET dynamics was proposed. The propagation of the bias into the binding was also evaluated by using simple ratio methods at equilibrium. Moreover, the analysis was additionally performed with the PRESTO reconstruction and compared to the vendor's 3D OP-OSEM. Quantification bias as a result of low counts in PET images reconstructed with the 3D OP-OSEM algorithm has been studied by several groups with special emphasis being placed on the impact of the bias on estimated activity concentrations and binding potentials in neuroreceptor studies (8-10, 16, 19, 26, 27). At low count rates, the distribution of the reconstructed events per voxel is asymmetric, leading to a bias in the mean of the voxel activity concentration values (9). MLEM

and OP-OSEM reconstructions tend to be biased in regions with low activity concentrations, particularly if these regions are surrounded by regions of high activity concentrations (16). Slambrouck et al., also demonstrated that regions with low activity concentrations will converge much more slowly and a very high number of iterations would be required to eliminate the positive bias (16). However, it is not usual to have a high enough number of iterations to avoid this convergence bias. Moreover, since there are other sources for bias apart from iteration numbers, a completely bias-free image is not possible (16) and at low count statistical levels, other factors, such as random estimation, can be critical. This is because single rates are not constant and/or the activity distribution is not static during the frame (at this point framing schemes should be carefully chosen). Previous works have reduced the random events estimation bias considerably by applying a reduction variance given by VRR algorithms (9, 14, 19). However, other factors, such as scatter overcorrection, global dead time correction instead of block-wise correction, inconsistences in the attenuation map, etc., can still contribute to the reconstruction bias. These factors are not within the scope of this work.

Other methods to reduce bias at low count rates have been proposed, e.g. Hong et al. (28) used a method called complementary frame reconstruction. This method involves the indirect formation of a low count image (short time frame) through the subtraction of two frames with longer acquisition times (high statistics). The short time frame is then excluded from the second, long frame data prior to reconstruction. The method was tested with a phantom and with clinical data using HRRT and Biograph mCT scanners and with OP-OSEM reconstruction. In contrast to this study, the authors focused their work on applications relating to estimation of the arterial input function, although they also commented on potential future applications. While, our alternative framing scheme, (Const Trues), is intended to mitigate the bias in any group of reconstructed

images, so far it was validated for equilibrium methods at low count rates and particularly for BI protocols when used together with ABP and simultaneously MR sequences. The goal here is to maximize the possibility to identify pre and post task effects together with other modalities and during the same brain conditions. In addition, it increases the possibility to detect binding differences by reducing the bias and keeping at the same levels during the pre-challenge and post-challenge time periods for a possible comparison. Since the bias cannot be avoided entirely, even when using 3D OP-OSEM + VRR reconstructions, we hypothesize that, if the bias is mainly due to the low count rates, the bias can be mitigated and maintained at a constant level by keeping the counts per frame constant during all PET dynamics (keeping bias constant for the all acquisition time interval).

The findings of our study support a previous bias investigation undertaken by Planeta-Wilson and colleagues using HRRT and OP-OSEM (MOLAR) reconstruction. Here, a bias of - 4 ± 2% was shown for GM (high activity concentration region) and 4 ± 5% for white matter (low activity concentration) regions (7). In terms of bias range, for low and high activity concentration regions, our results showed agreement, since the bias range values were closer for BG (with ± 3%) and Hot_1 (between -3% and 5%) with respect to activity concentration accuracy. In addition, based on data obtained from a ^{11}C filled decay phantom study and a human data (slopes), we also observed a negative bias for high activity concentration regions when the frame length was shortened (low counts). Our study differs from previous studies reported in the analysis approach since we additionally evaluated the slope changes from a complete dynamic PET acquisition rather than just a single frame with different count statistics. Furthermore, our results completely diverged from others in terms of the amount of bias found. Johansson et al., reported a significantly higher bias which was in the range of -16% to -18% in high activity concentration regions (1M

and 200k counts, respectively) using HRRT and 3D OP-OSEM. van Velden et al., reported a bias of around - 9% to - 14% in GM (Hoffman phantom in 5 seconds frame) using the same scanner and reconstruction (5, 19). Moreover, Reilhac and colleagues reported a bias of up to 80% in the CER region for the end of the activity time course in simulations using 3D UW-OSEM (8).

It is important to interpreter these results carefully since our study differs in some aspects, for example, in terms of the activity concentration and high to low activity concentration ratios used, the radioisotope and radiopharmaceuticals, and the range of analyzed statistics. Moreover, there are some configuration differences between scanners and the 3D OSEM reconstruction procedures presented (number of iterations and subsets), post-processing smoothing, etc. However, in the interest of comparability, we tried to compare our results with the closest 3D OP-OSEM procedures and statistics as possible.

In terms of bias propagation into binding values, our study is in agreement with van Velden et al (19), where a bias of - 14% BP_{ND} was reported when using reference tissue models. In our study, a BP_{ND} bias of up to - 40% ± 6% per hour (Const 2 min) was found and when mitigated with the Const Trues framing scheme, the bias was -7% ± 5% per hour in ACC (observed as slopes in the human data example, see in Table 6). It is important to emphasize that our approach is based on BI studies and the BP_{ND} values in other studies were obtained from bolus only analysis applying kinetic modeling instead of simple ratio methods. We hypothesize, that pure bolus and pure infusion studies may suffer from bias issues similar to those found in our study and that it might be possible to mitigate the bias with the proposed Const Trues framing approach. As the bias is introduced during iterative image reconstruction, parameters estimated via kinetic modeling will potentially be affected as well. However, further studies for evaluating this are needed.

509 The slopes approach was used in this study because we expected a more similar bias
510 between time intervals (T4, T5 and T6) and along the TACs when applying the Const Trues
511 framing scheme. In this case, the slope should not be changed by the bias. Nevertheless, bias
512 between subjects can. We noticed the same trend as found in the ^{11}C filled phantom decay study,
513 where the bias became negative along the TAC, especially in time interval T6. Furthermore, it was
514 also possible to identify a stronger bias in a smaller region with high activity concentration,
515 represented by Hot_2 (simulating nucleus accumbens volume). Unfortunately, this region showed
516 consistently larger bias values, especially for BP. The negative bias for activity concentration was
517 in the 1% to -8% range, and the variability was higher between the different time intervals (T4, T5
518 and T6) leading to larger BP mean bias values of up to - 10%. The high BP bias values and its high
519 variability for regions comparable to Hot_2 in size could cause spurious results during neuroreceptor
520 study analysis. Walker and colleagues (9) found -13% without VRR and -5.5% with VRR bias (for
521 1.7M counts) in the caudate head (1.3 ml) which is of similar size to Hot_2 (1.13 ml).

522 It should also be noted, that the negative trend of bias in hot regions and the positive trend
523 of bias in the BG region leads to an amplified underestimation of BP (Equation 3). This is an
524 important point of consideration for neuroreceptor studies using equilibrium conditions, especially
525 if the aim of the study is to evaluate the binding prior, during, and post a specific task. This holds
526 especially for cognitive tasks where the potentially induced effects are caused by endogenous
527 release and are thus expected to be smaller than pharmacological tasks (e.g. video game playing
528 tasks with [^{11}C]raclopride, 13% BP decrease versus psychostimulants 10% to 20% BP decrease
529 (29)). In such a case, the bias could mask the effect in the Hot_1 region, since it would be larger than
530 10% during the time interval T4 and 5% during the time interval T6, when a scheme with Const
531 frames is used (see in Figure 4). This effect can also be observed for ABP in-vivo TACs (see

Figure 6, Figure 7 and Table 3). Here, we observed a relative change of up to - 40% per hour in the ACC region with the vendor's 3D OP-OSEM reconstruction and with the Const 2 min framing scheme. This could lead to misinterpretation of the effects caused by the task and give rise to incorrect conclusions. With the proposed, alternative Const Trues framing scheme, the average BP bias could be reduced/mitigated to mean values around 5% in the phantom study (see Figure 8) which is constant for all intervals T4, T5, and T6. A drawback of the proposed framing method is the use of the very short time frames at the beginning of the acquisition, which result from the reference counts number in the last frame. This also leads to an increased variability (Figure 8). Nevertheless, the time required to reach equilibrium in neuroreceptor studies, e.g. for ABP usually starts at around 30 minutes p.i., so this drawback is tolerable for our studies, since the relevant part of the PET study is during the equilibrium phase interval (see Table 6). Note that the SE values remain constant with our Const Trues framing scheme (Figure 7 and Figure 10).

For the Incr 2-3-5 min framing, a reduction in the BP mean bias values was also observed. However, regarding the difference between time intervals T4, T5 and T6, a higher bias (around 10%) can be seen in T4 for Incr schemes compared to Const Trues (around 5% from T4 to T6). From these findings, framing schemes with constant frame lengths are less suitable for the evaluation of BP_{ND} when is required for the analysis prior and post effects in neuroreceptor studies as the bias range has high variability between the time intervals (from T4 = 15% to T6 = 5%). In Figure 5, the falling and rising trends of the bias for the BG region and the falling behavior of the bias for the hot regions can be clearly observed for all studied framing schemes. The similar results were found for the TACs in the human brain study with [^{11}C]ABP688 (especially the rising behavior in the last time interval for CER and falling behavior for ACC, see Figure 6). This finding

554 was also noticed by van Velden et. al. (19) using reference region (pons) approaches with
555 [^{11}C]Flumazenil.

556 When comparing different reconstructions procedures, PRESTO showed slightly lower bias values
557 for regions with low activity concentration (BG and CER) and rising trends, which were smaller,
558 compared to the vendor´s 3D OP-OSEM (especially for Const frame schemes). Furthermore, when
559 using PRESTO for the phantom study, lower slope values (relative change per hour) were noticed
560 in the time interval T6 for the BG VOI compared to the vendor´s 3D OP-OSEM reconstruction.
561 However, when evaluating the accuracy of the BP values for both reconstructions, the remaining,
562 optimized bias was around 5% for the vendor´s 3D OP-OSEM compared to around 10% for
563 PRESTO with the Const Trues. We attribute this difference to the crosscalibration between
564 PRESTO and the vendor's 3D OP-OSEM reconstruction. The PRESTO reconstruction lead to a
565 slightly smaller bias for low activity concentration regions during the final time interval (T6) in
566 the ^{11}C filled phantom decay study. For the ABP TACs, a smaller range of the relative change per
567 hour and bias values closer to zero were observed with PRESTO in the low activity concentration
568 regions when compared to the vendor's 3D OP-OSEM reconstruction for all tested framing
569 schemes.

570 In summary, all framing schemes methods, even with the minimized bias range due to our
571 proposed framing scheme Const Trues, produce a bias of at least 5%, which should be taken into
572 account for the conclusions drawn from the observed BP_{ND} values. Moreover, when task effects
573 are evaluated with the mitigated bias framing scheme (Const Trues), the task must induce a change
574 sufficiently larger than 5% in order to be observable in equilibrium studies with ABP during the
575 analyzed time interval.

Further studies are planned to investigate the influence of scatter correction at low count rates, as it has already been pointed out by Jian and colleagues (10) that scatter correction is a potential bias source.

Conclusion

This work aimed to analyze the bias in activity concentrations estimated from PET images and its propagation into binding potential values for equilibrium studies using a ^{11}C filled decay phantom study and a human data set from a BI study with ABP. Taking into account all framing schemes tested, one can conclude that PRESTO showed lower bias values for the low activity concentration region, particularly when using the Const Trues framing scheme method proposed. Therefore, in order to be observable, the size of any potentially endogenous response to tasks or challenges in neuroreceptor studies with ABP using the BI protocol should be sufficiently larger than 5% for our proposed framing scheme and when using vendor's reconstruction, since the bias propagates into the biding potential values. Further studies are required to estimate the bias introduced by other sources, such as scatter correction.

Declaration

Ethics Approval and Consent to Participate

Our work has been carried out in accordance to The Code of Ethics of the World Medical Association (Declaration of Helsinki) for experiments. All participants (human example) signed written informed consents in addition to verbal consent. The privacy rights of human subjects were observed. The ICMJE Recommendations for the Conduct, Reporting, Editing, and Publication of Scholarly Work in Medical Journals have been followed.

Consent for Publication

All authors had full access to all data in the study. We confirm that the manuscript has been read and approved for submission by all the named co-authors.

Availability of data and materials

The datasets used and analyzed during the current study are available from the corresponding author on reasonable request.

Disclosure/Competing Interests

These data are part of the Dr. rer. medic. thesis at the Medical Faculty of the RWTH Aachen University, Germany of Cláudia Régio Brambilla. No potential conflict of interest relevant to this article was reported.

Funding

This work was supported in part by the EU-FP7 funded project TRIMAGE (Nr. 602621), and Cláudia Régio Brambilla thanks to DAAD for financial support (Nr. 57299294).

Author contributions

CRB: PET bolus-infusion protocol optimization, data acquisition, PET imaging data analysis, statistical design and analysis, manuscript writing, correction and revision. *JS:* PET reconstruction discussions, PRESTO reconstruction, manuscript revision and correction. *AI:* script for PET True events curve extraction and manuscript revision. *LT:* MR-PET hardware and data acquisition. *HH:* PET study design discussions, revision and corrections of the manuscript. *ERK:* MR-PET attenuation correction and revision of the manuscript. *NJS:* MR-PET hardware and revision of the manuscript. *IN:* ABP study design and setup, approval ethics and BfS and revision of the

manuscript. *CL:* study design and setup, data analysis revision, manuscript corrections and revision.

Acknowledgment

The authors thank to Magdalene Vögeling, Cornelia Frey, Silke Frensch and Suzanne Schaden for their technical assistance in data acquisition. The authors would like to thank Markus Lang and Stefan Stüsgen for the [^{11}C]ABP688 production and Dr. Andreas Matusch for the implementation of the metabolite correction method and support in the equilibrium analysis for the human study. Finally, the authors would like to thank Claire Rick for proofreading the manuscript.

References

1. Shepp LA, Vardi Y. Maximum likelihood reconstruction for emission tomography. IEEE Trans Med Imaging. 1982;1(2):113-22.
2. Hudson HM, Larkin RS. Accelerated image reconstruction using ordered subsets of projection data. IEEE Trans Med Imaging. 1994;13(4):601-9.
3. Barrett HH, White T, Parra LC. List-mode likelihood. J Opt Soc Am A Opt Image Sci Vis. 1997;14(11):2914-23.
4. Liu X, Comtat C, Michel C, Kinahan P, Defrise M, Townsend D. Comparison of 3-D reconstruction with 3D-OSEM and with FORE plus OSEM for PET. Ieee T Med Imaging. 2001;20(8):804-14.
5. Johansson J, Clikonen V, Teraes M. Quantitative brain imaging using the new, fast iterative histogram-mode reconstruction for the HRRT PET scanner. Ieee Nucl Sci Conf R. 2007:3463-7.
6. van Velden FH, Kloet RW, van Berckel BN, Lammertsma AA, Boellaard R. Accuracy of 3-dimensional reconstruction algorithms for the high-resolution research tomograph. J Nucl Med. 2009;50(1):72-80.
7. Planeta-Wilson B, Yan J, Mulnix T, Carson RE. Quantitative Accuracy of HRRT List-mode Reconstructions: Effect of Low Statistics. IEEE Nucl Sci Symp Conf Rec (1997). 2008;2008:5121-4.
8. Reilhac A, Tomei S, Buvat I, Michel C, Keheren F, Costes N. Simulation-based evaluation of OSEM iterative reconstruction methods in dynamic brain PET studies. Neuroimage. 2008;39(1):359-68.
9. Walker MD, Asselin MC, Julyan PJ, Feldmann M, Talbot PS, Jones T, et al. Bias in iterative reconstruction of low-statistics PET data: benefits of a resolution model. Phys Med Biol. 2011;56(4):931-49.
10. Jian Y, Planeta B, Carson RE. Evaluation of bias and variance in low-count OSEM list mode reconstruction. Phys Med Biol. 2015;60(1):15-29.
11. Comtat C, Bataille F, Michel C, Jones JP, Sibomana M, Janeiro L, et al. OSEM-3D reconstruction strategies for the ECAT HRRT. Ieee Nucl Sci Conf R. 2004:3492-6.
12. Cloquet C, Defrise M. MLEM and OSEM Deviate From the Cramer-Rao Bound at Low Counts. IEEE Transactions on Nuclear Science. 2013;60(1):134-43.
13. Chen TB, Lu HHS, Kim HK, Son YD, Cho ZH. Accurate 3D reconstruction by a new PDS-OSEM algorithm for HRRT. Radiat Phys Chem. 2014;96:107-14.
14. Byars LG, Sibomana M, Burbar Z, Jones J, Panin V, Barker WC, et al. Variance reduction on randoms from delayed coincidence histograms for the HRRT. 2005 Ieee Nuclear Science Symposium Conference Record, Vols 1-5. 2005:2622-6.
15. Watson CC. New, faster, image-based scatter correction for 3D PET. Ieee T Nucl Sci. 2000;47(4):1587-94.
16. Van Slambrouck K, Stute S, Comtat C, Sibomana M, van Velden FH, Boellaard R, et al. Bias reduction for low-statistics PET: maximum likelihood reconstruction with a modified Poisson distribution. IEEE Trans Med Imaging. 2015;34(1):126-36.
17. Scheins JJ, Herzog H, Shah NJ. Fully-3D PET image reconstruction using scanner-independent, adaptive projection data and highly rotation-symmetric voxel assemblies. IEEE Trans Med Imaging. 2011;30(3):879-92.

18. Herzog H, Langen KJ, Weirich C, Rota Kops E, Kaffanke J, Tellmann L, et al. High resolution BrainPET combined with simultaneous MRI. Nuklearmedizin. 2011;50(2):74-82.
19. van Velden FH, Kloet RW, van Berckel BN, Wolfensberger SP, Lammertsma AA, Boellaard R. Comparison of 3D-OP-OSEM and 3D-FBP reconstruction algorithms for High-Resolution Research Tomograph studies: effects of randoms estimation methods. Phys Med Biol. 2008;53(12):3217-30.
20. Association NEM. NEMA Standards Publication NU 2-2007: Performance Measurements of Positron Emission Tomographs: National Electrical Manufacturers Association; 2007.
21. McCollum LA, Walker CK, Roche JK, Roberts RC. Elevated Excitatory Input to the Nucleus Accumbens in Schizophrenia: A Postmortem Ultrastructural Study. Schizophrenia Bulletin. 2015;41(5):1123-32.
22. Regio Brambilla C, Veselinovic T, Rajkumar R, Mauler J, Orth L, Ruch A, et al. mGluR5 receptor availability is associated with lower levels of negative symptoms and better cognition in male patients with chronic schizophrenia. Hum Brain Mapp. 2020.
23. Elmenhorst D, Mertens K, Kroll T, Oskamp A, Ermert J, Elmenhorst EM, et al. Circadian variation of metabotropic glutamate receptor 5 availability in the rat brain. J Sleep Res. 2016;25(6):754-61.
24. Kops ER, Herzog H, Shah NJ. Comparison template-based with CT-based attenuation correction for hybrid MR/PET scanners. EJNMMI Phys. 2014;1(Suppl 1):A47.
25. Ametamey SM, Treyer V, Streffer J, Wyss MT, Schmidt M, Blagoev M, et al. Human PET studies of metabotropic glutamate receptor subtype 5 with 11C-ABP688. J Nucl Med. 2007;48(2):247-52.
26. Belanger MJ, Mann JJ, Parsey RV. OS-EM and FBP reconstructions at low count rates: effect on 3D PET studies of [C-11] WAY-100635. Neuroimage. 2004;21(1):244-50.
27. Haggstrom I, Axelsson J, Schmidtlein CR, Karlsson M, Garpebring A, Johansson L, et al. A Monte Carlo study of the dependence of early frame sampling on uncertainty and bias in pharmacokinetic parameters from dynamic PET. J Nucl Med Technol. 2015;43(1):53-60.
28. Hong I, Cho SH, Michel CJ, Casey ME, Schaefferkoetter JD. Complementary frame reconstruction: a low-biased dynamic PET technique for low count density data in projection space. Physics in Medicine and Biology. 2014;59(18):5441-55.
29. Laruelle M. Imaging synaptic neurotransmission with in vivo binding competition techniques: a critical review. J Cereb Blood Flow Metab. 2000;20(3):423-51.

List of Abbreviations

[^{11}C]ABP688 - (3-(6-methyl-pyridine-2-ylethynyl)-cyclohex-2-enone-O-[11C]-methyloxime)

3D OP-OSEM - 3D Ordinary Poisson Ordered Subset Expectation Maximization

ACC – Anterior Cingulate Cortex

BG - background region

BI - Bolus plus Infusion

BP - Binding Potential – related to phantom data in this work

BP_{ND} – non-displaceable Binding Potential – related to human data in this work

CER – Cerebellum

EEG - electroencephalography

GM - grey matter cortex

LOR – Line of Response

mGluR5 – metabotropic glutamatergic receptor type 5

ML-EM - Maximum Likelihood - Expectation Maximization

MR – Magnetic resonance

PET – Positron Emission Tomography

Post_Tl – Posterior Temporal Cortex

PVE – Partial Volume Effect

SE – Standard Error

SSS – Single Scatter Simulation

TAC – Time Activity Curve

VOI - volume of interest

VRR – Variance Reduction Algorithm

Figures

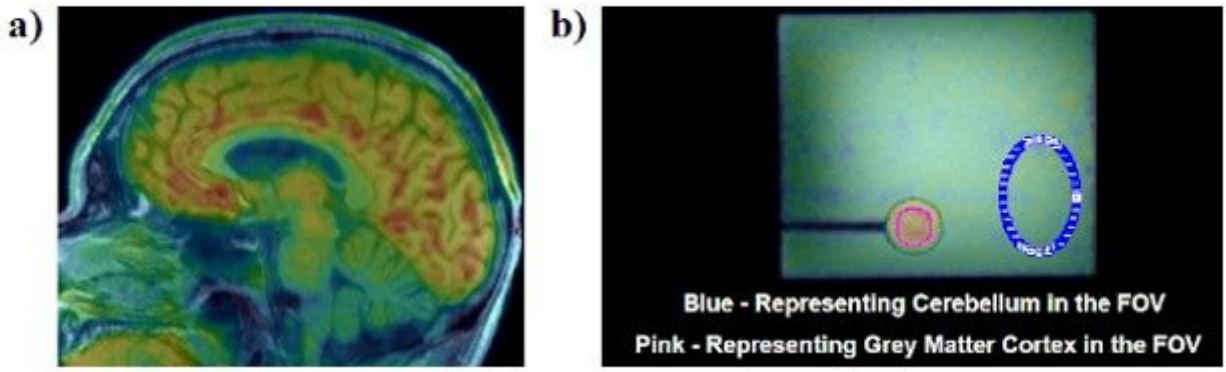

Figure 1

a) Sagittal PET image from the ABP study overlaid with MR T1 image and b) Sagittal PET image of the NEMA phantom overlaid with an MR T1 image during the 11C filled phantom decay study. The high activity concentration region (pink VOI) and low activity concentration region (blue VOI) is highlighted for bias analysis.

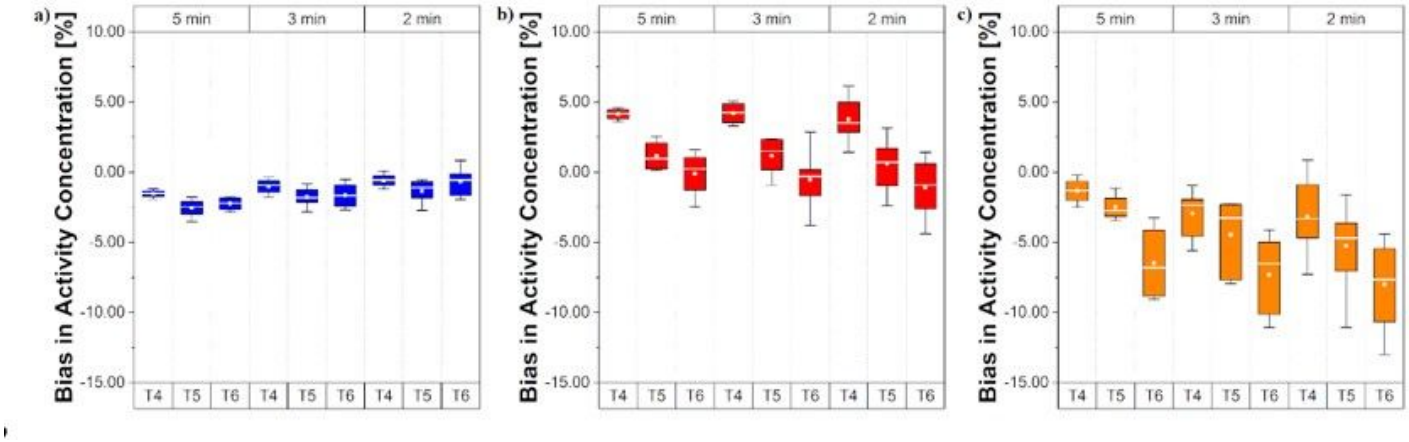

Figure 2

Bias and variability in activity concentration for a) BG region (low activity concentration), b) Hot1 region (high activity concentration) and c) Hot2 region (high activity concentration); all with vendor's reconstruction.

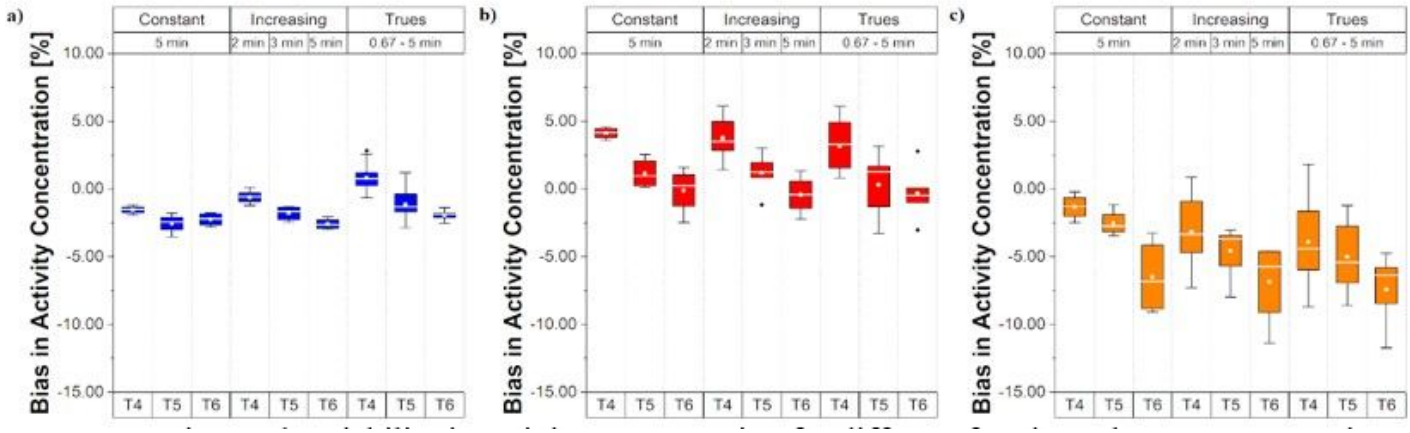

Figure 3

Bias and variability in activity concentration for different framing schemes a) BG region (low activity concentration), b) Hot1 region (high activity concentration) and c) Hot2 region (high activity concentration); all with vendor's 3D OP-OSEM reconstruction.

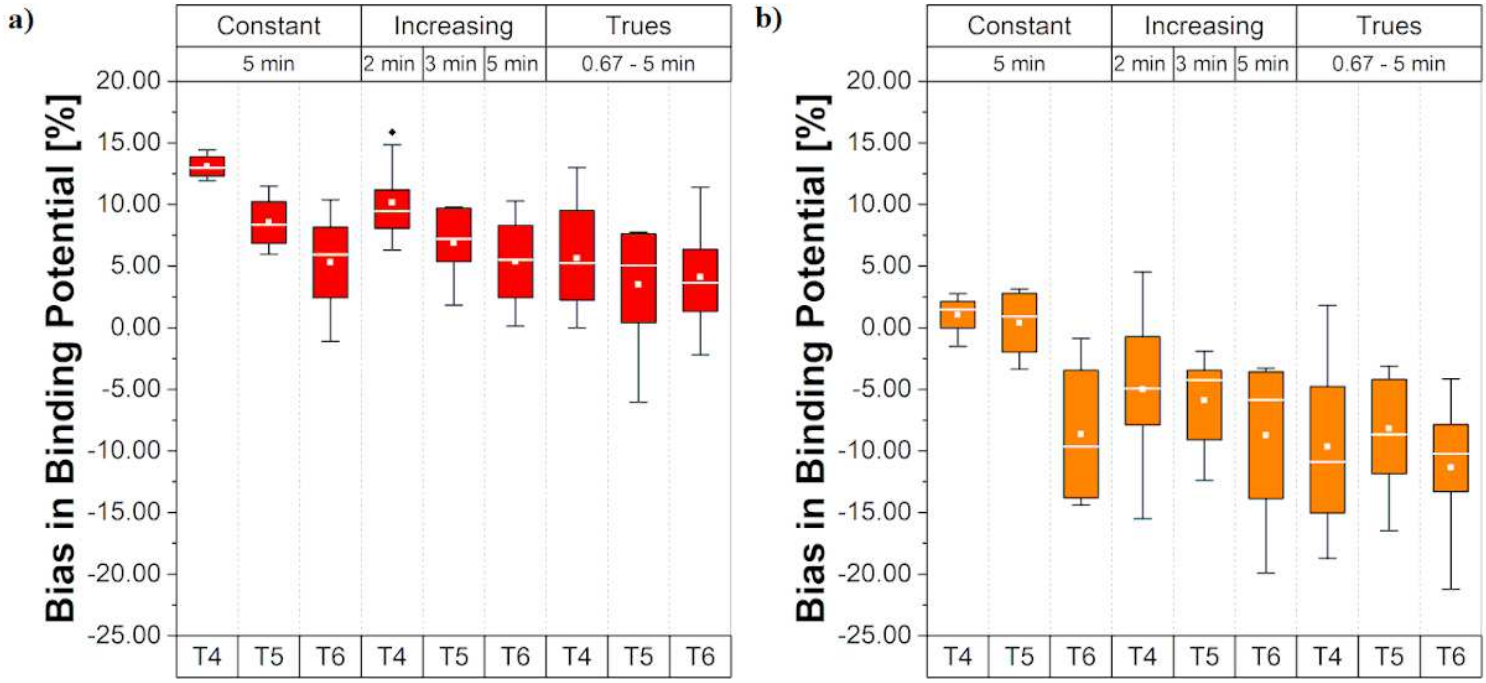

Figure 4

Bias and variability of BP values for a) Hot1 region, and b) Hot2 region; all with vendor's 3D OP-OSEM reconstruction.

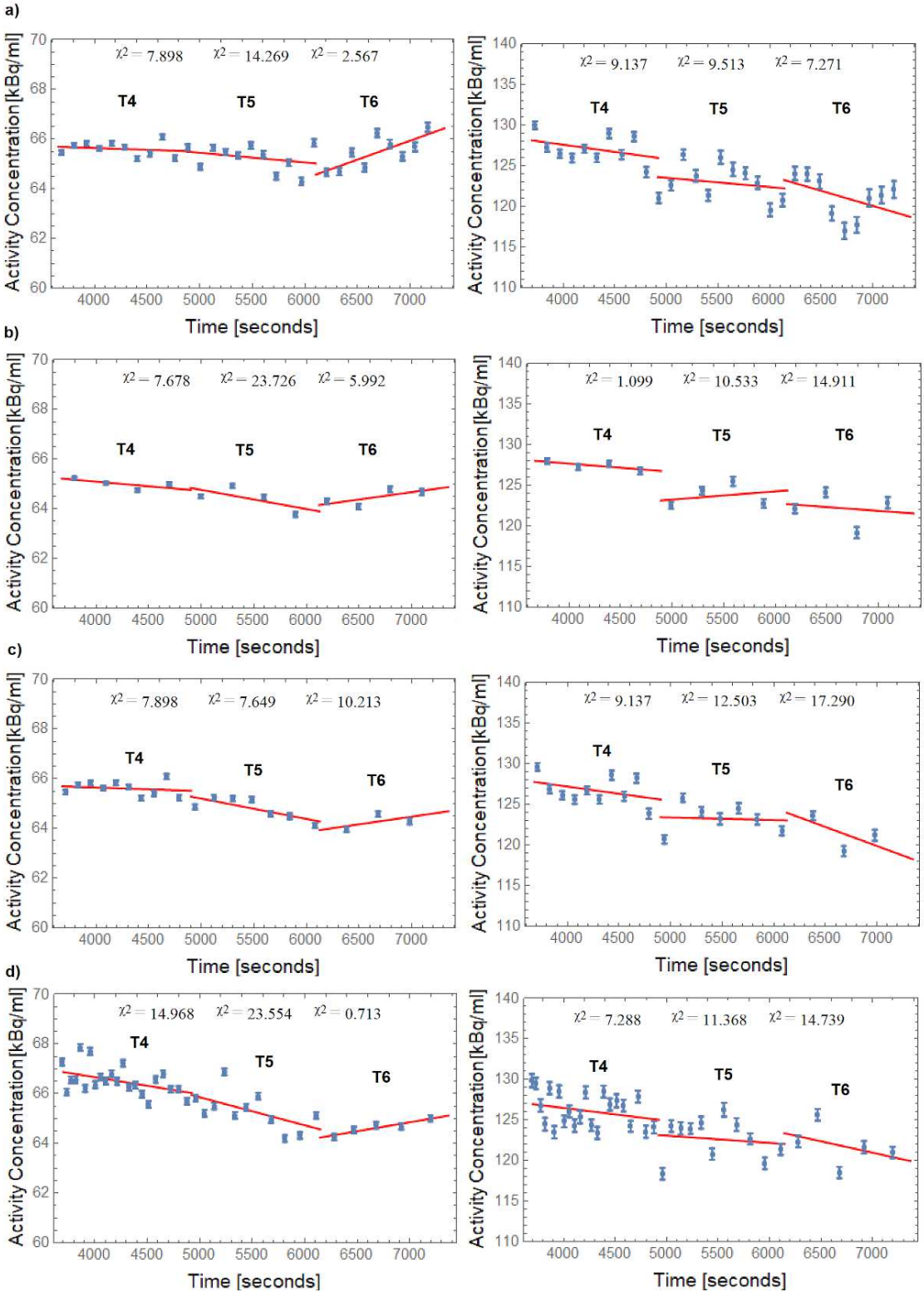

Figure 5

TACs and linear fits for BG (left side) and Hot1 (right side) regions for a) Const 2min, b) Const 5min, c) Incr 2-3-5 min and d) Const Trues; all with vendor's 3D OP-OSEM reconstruction. 2: goodness of linear fit.

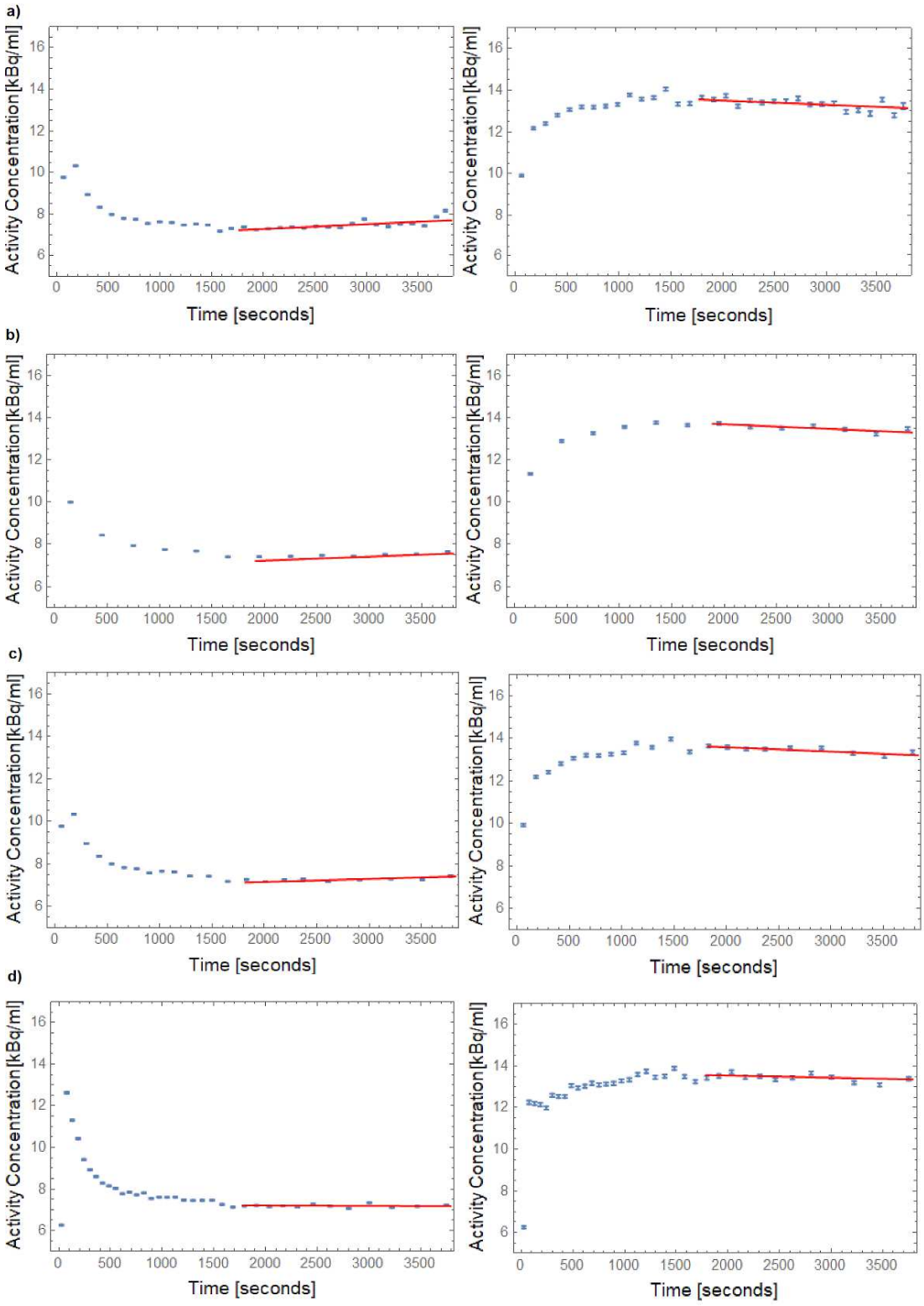

Figure 6

TACs and linear fits during equilibrium in CER (left side) and ACC (right side) regions from a human brain study for a) Const 2 min, b) Const 5 min, c) Incr 2-3-5 min and d) Const Trues; all with vendor's 3D OP-OSEM reconstruction.

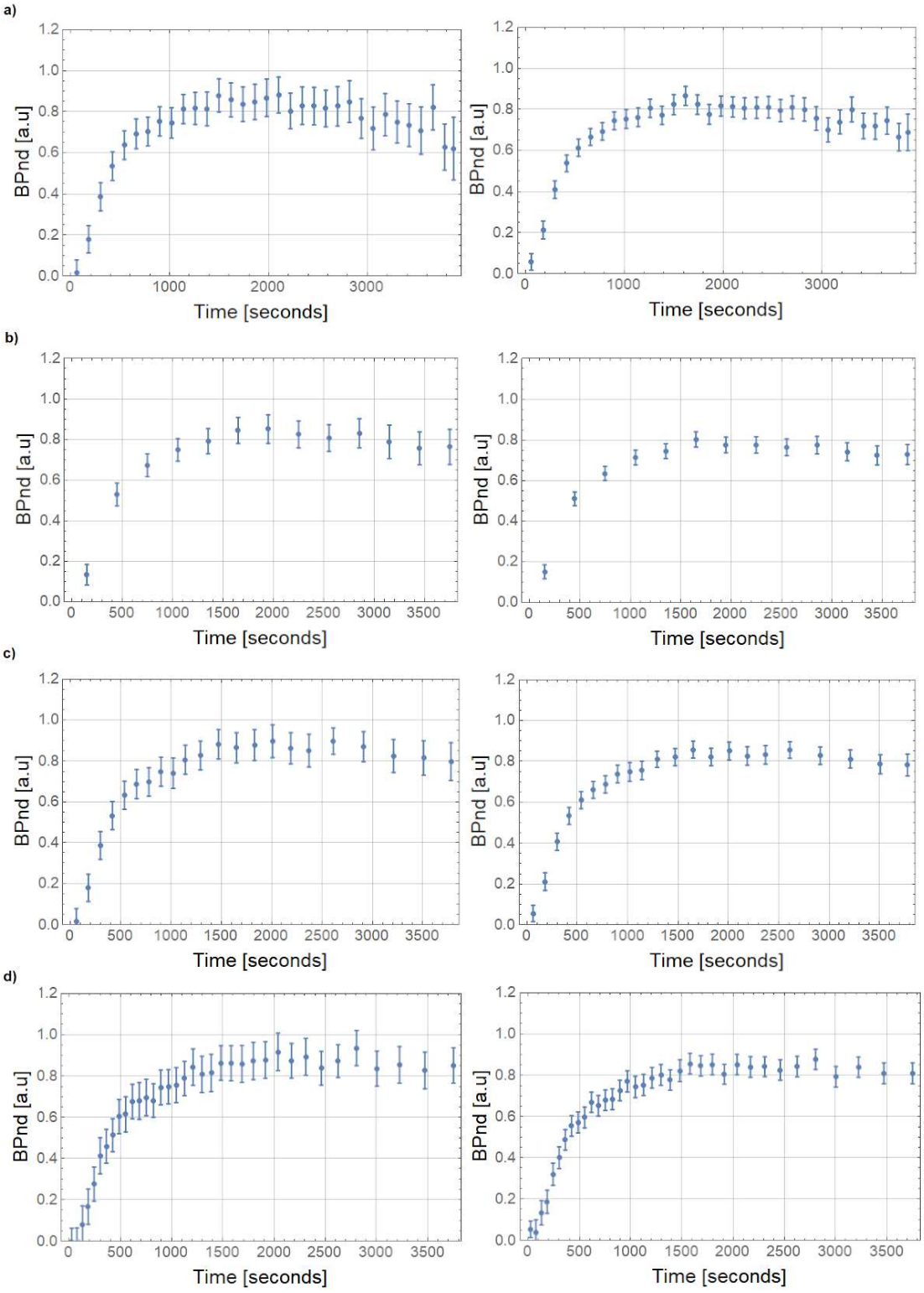

Figure 7

Values of BPND ± SE for ACC (left side) and Post-TI (right side) in a human brain study for a) Const 2 min, b) Const 5 min, c) Incr 2-3- 5 min and d) Const Trues; all with vendor´s 3D OP-OSEM reconstruction.

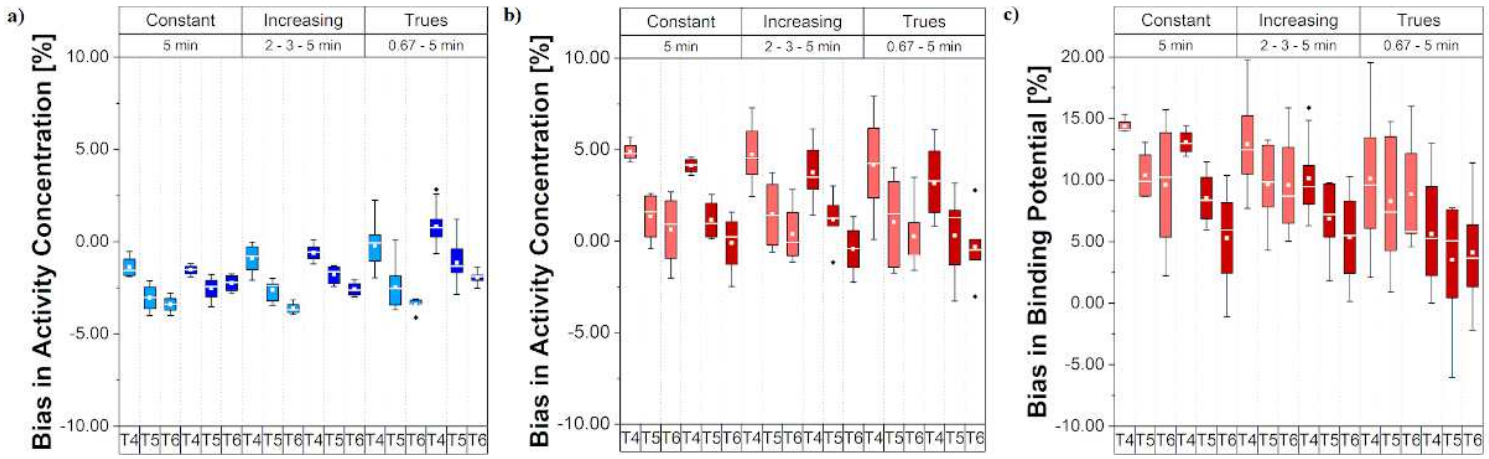

Figure 8

Bias in activity concentrations and BP values for different framing schemes comparing PRESTO (light blue, light red) and vendor's 3D OP-OSEM (dark blue, dark red) in a) BG, b) Hot1 and c) Hot1 BP.

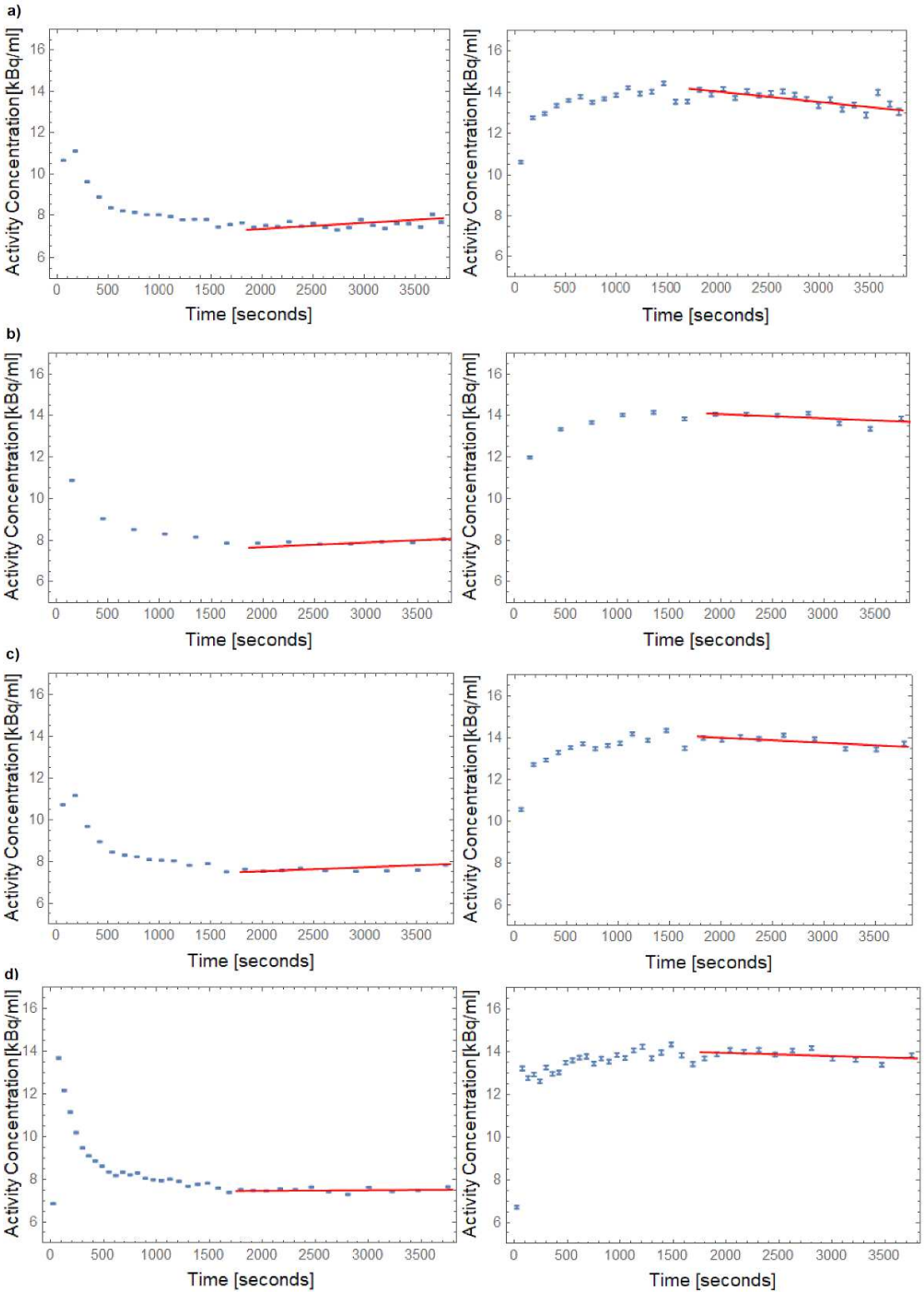

Figure 9

TACs and linear fits during equilibrium in CER (left side) and ACC (right side) regions from a human brain study for a) Const 2 min, b) Const 5 min, c) Incr 2-3-5 min and d) Const Trues; all with PRESTO reconstruction.

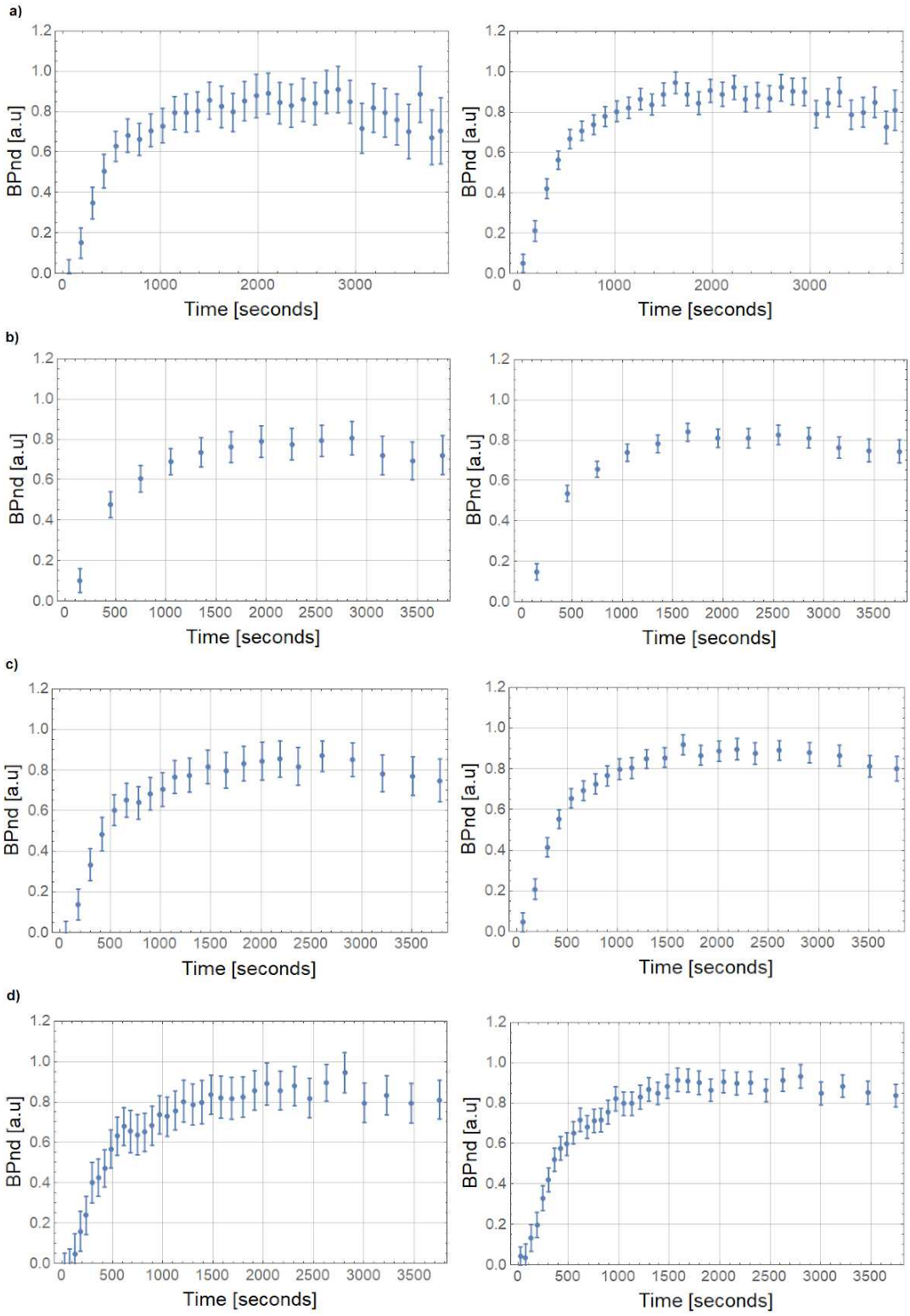

Figure 10

Values of BPND ± SE values for ACC (left side) and Post-TI (right side) regions from a human brain study for a) Const 2 min, b) Const 5 min, c) Incr 2-3-5 min and d) Const Trues; all with PRESTO reconstruction.

Supplementary Files

This is a list of supplementary files associated with this preprint. Click to download.

- Supplement.docx